FEDERATED LEARNING FOR IMAGE CLASSIFICATION BASED ON DEEP LEARNING

by

Khanh Le Dinh Viet (K.L.D.V.)

Khiem Le Ha (K.L.H.)

THE FPT UNIVERSITY HO CHI MINH CITY

FEDERATED LEARNING FOR IMAGE CLASSIFICATION BASED ON DEEP LEARNING

by

Khanh Le Dinh Viet (K.L.D.V.)

Khiem Le Ha (K.L.H.)

Supervisor:

M.S. Trung Nguyen Quoc

A final year capstone project submitted in partial fulfillment of the requirement for the Degree of Bachelor of Artificial Intelligent in Computer Science

DEPARTMENT OF ITS

THE FPT UNIVERSITY HO CHI MINH CITY

March 2023

ACKNOWLEDGMENTS

We would like to give a big thanks to our supervisor M.S. Trung Nguyen Quoc for many valuable guidance throughout our progress. He also dedicated his time to revising our experiment results and the final report.

AUTHOR CONTRIBUTIONS

Methodology direction, K.L.D.V and K.L.H.; Dataset preparation, K.L.D.V.; Dataset preprocessing, K.L.D.V; Algorithm collection, K.L.H.; Framework establishment, K.L.H.; Experiments, K.L.D.V; Results analysis, K.L.D.V; Report writing, K.L.H; Support materials, figures and appendix, K.L.D.V; Report revision, K.L.D.V and K.L.H. All authors have read and agreed to the Final Capstone Project document.

ABSTRACT

Federated Learning has been emerged as a promising for modern Machine Learning techniques. Classical manner of operating in a centralize dataset come up against critical privacy issues. Beside that real data reacted with real user's behavior is beneficial to tasks which involve model to be trained on practical data. For example, language model can be leveraged by playing on user data emitted while they text for speech recognition or next word prediction tasks. We could also utilize images on end devices to improve image classification models. Two current state-of-the-art methods when dealing with federated system are **FedAvg** and **FedProx.** While **FedAvg** proposed a heuristic algorithm that is quite robust about independent and identically distributed distribution (**IID**), the latter further upgrade upon the local loss setting for stability with respect to the **non-IID** distribution. There are two main nature challenges within the task as indicated in **FedProx** work: system heterogeneity and statistical heterogeneity. One more difficulty: the lack of a systematic hyperparameters tuning as well as model selection approach. **FedAvg** and **FedProx** mostly work with canonical datasets and their synthesis variants like **MNIST, CIFAR-10**. In this work, we employ the Federated Learning approaches to unusual dataset to observe the capabilities of generalizing when handling domain-specific tasks. Concretely, we adopt **FedAvg** and **FedProx** on: (1) a brain tumor dataset with 3064 512×512 T1-weight images and (2) a **VNPlant-200** dataset which includes 20,000 images of 200 unique medicinal plants. Following the work in **FedAvg** and **FedProx,** two algorithms are applied with a careful hyperparameter tuning and inspect the effect of federated setting on the decentralized environment. The work empirically demonstrates the impact of federated learning on distinct domains. In addition, the experiments provide a heuristic scheme for hyperparameter controlling in other similar tasks or data, in this case, distributed model training and brain tumor or medicinal plant datasets.

Keywords: Federated Learning; FedAvg; FedProx; Distributed Training; Brain Tumor; Medicinal Plant; VGG16; ResNet50; ConvNext; MaxViT

CONTENTS

List of Figures

List of Tables

List of Abbreviations

FL	*Federated Learning*
AI	*Artificial Intelligence*
NLP	*Natural Processing Language*
SR	*Speech Recognition*
CV	*Computer Vision*
ML	*Machine Learning*
GDPR	*General Data Protection Regulation*
HFL	*Horizontal Federated Learning*
VFL	*Vertical Federated Learning*
FTL	*Federated Transfer Learning*
IID	*Independent and identically distributed*
CNN	*Convolutional Neural Network*
SGD	*Stochastic Gradient Descent*
GD	*Gradient Descent*
LRN	*local responses normalization*
ViT	*Vision Transformers*
CLAHE	*Contrast Limited Adaptive Histogram Equalization*

1. INTRODUCTION

1.1 Modern Artificial Intelligence Technologies and Big Data Era

The growth of Artificial Intelligence (**AI)** applications has been progressively supported by vast amounts of data [1], [2]. Conventionally, **AI**-related applications often fall into ordinary categories like computer vision (**CV**), natural processing language (**NLP**), speech recognition (**SR**). Those are also the most important appliances of **AI** in real world. Sometimes, the model can outperform human performance. For example, Deep Learning-based face recognition can achieve exceptional levels of performance given millions of training samples [3], [4]. These systems obviously require huge a bunch of data to gain satisfying levels of results due to the complexity of the model's architecture.

Generally, the big data system demands special methods in gathering and processing because data regularly comes on a small scale. In addition, data diversity mostly appears as a critical adversity to confront with. Missing values, missing labels, disparity distribution largely expect big effort from domain experts to repairing. In fact, benchmark datasets used within standard tasks usually require an enormous work in selectively gathering, processing and thus need to be done in a proper and comprehensive research than the work evaluate on it [5]–[7]. Some demands raised in the context of narrower domains now show that it is hungry for data, precisely large-scale data to come up with training.

End user's data turns out to be a great source of data for **ML** tasks. This kind of data holds a very important nature: it is the real data that is eventually assessed and consumed by the final trained model. The modern world currently has serious concerns regarding data privacy and data ownership: which org has the ability and the rights to use data for building **AI** technologies. Some university labs or specific firms developing their **AI** research or products adopt their own business data or data that they created by themselves which is in this situation they have the full ownership over this data. But things get complicated in certain fields: data exists in various forms, generated by different parties and the naïve approach would be transfer data

into one central location and perform plenty of **ML** techniques. However, this method is no longer valid today. Owners of data are aware of their privacy rights, and they do not want their private information to be used illegally for commercial or political purposes.

Strict controls on data collection and data usage have likewise been imposed by law makers. General Data Protection Regulation (**GDPR**) issued by European Union in 2018 is a concrete example. Under this restrictive landscape, gathering and sharing data among separate organizations is becoming more and more difficult.

Even when we have a valid procedure dedicated to passing sensitive data around silos for training **AI** models, there are two more challenges. First, the benefit of data collaboration is not clear, or at least it is hard to measure if the procedure follows a super rigid manner, e.g., encrypting and shuffling all the data before entering the training phase. The fear of losing control over data and the lack of transparency make the crucial trade-off consideration from the owner's perspective. Second, some data have severe sensitive nature that cannot be moved from the owner's location, e.g., medical records and financial transactions, hence prohibit free data circulation.

How to solve this privacy problem is mandatory as the rules will progressively more rigorous. **AI** community has been witnessed tremendous of notable breakthroughs in ten years since 2012 due to the development hardware strengths and large-scale training datasets. An **AI** winter is going to happen if this situation is not sufficiently addressed.

1.2 Federated Learning as an enhanced solution

Federated Learning (**FL**) relies on a pure idea that lets the model being trained in-place at the data location, which we refer as local data or device's data. Then the information about trained model (weights or gradients) is the quantity that moving around for assembling the well-behaved application. The detailed explanation would be data reside at its own location, and some variable amount of update, i.e., training and validation, are executed. Conventionally, the method works like server-client architecture where there is a global model located at the server device and each client carries its dataset. Proper confidentiality plays an integral role

on securing the inner content or sometimes the inherent nature of data being transferred. Furthermore, the communication process also differs among several leading implementation which affects different desired optimal goals in different ways.

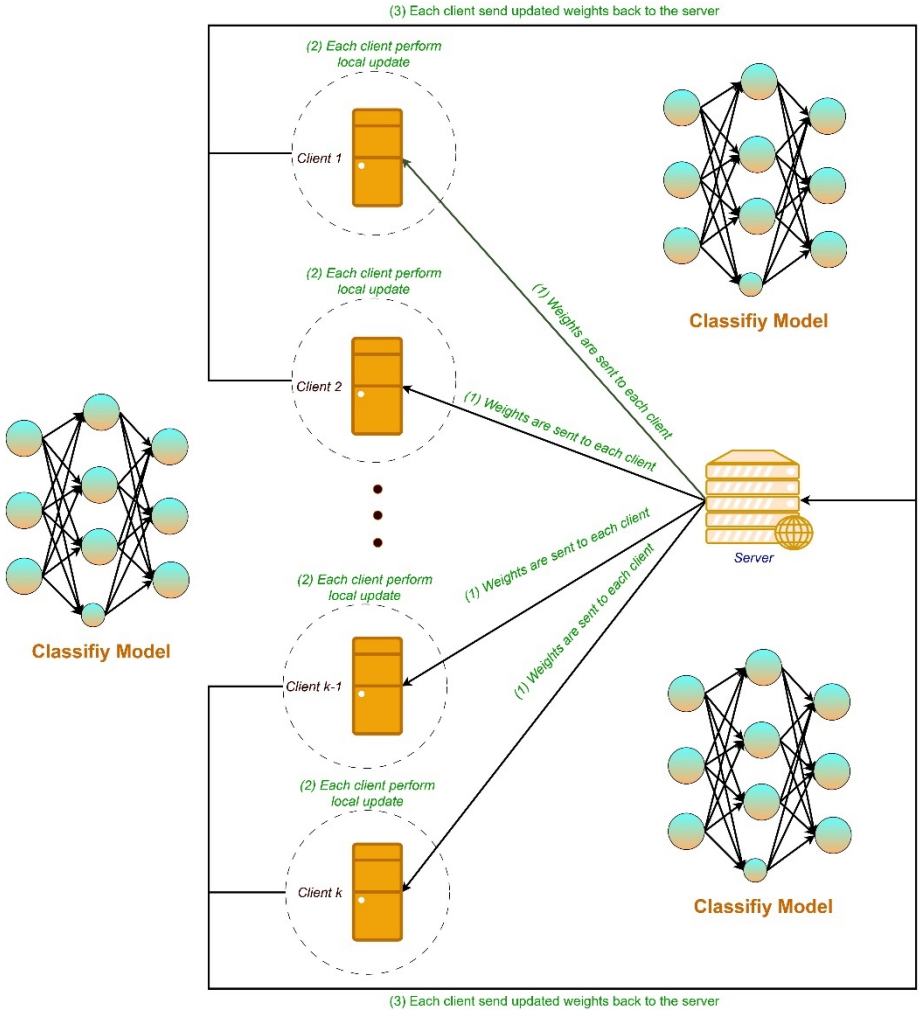

Figure 1. An example of **FL** algorithm

FL concepts first evolve in a decent form in 2016 in [8], namely **FedAvg**. The authors proposed an iterative approach for jointly updating the global model throughout communication rounds. As described above, in this federated scheme does not compel a whole centralize dataset at one place, as well as data at each device to be sent back-and-forth. To be more detailed, for several updates, under encryption, clients send local model parameters which then be used to incorporate into a new stateful global model representing current trained model given a passed number of rounds. Note that this is a repetitive training design. One thing can be theoretically

assured from a particular client view: its data is not revealed or examined common patterns with other clients or the server.

Horizontal Federated Learning (**HFL**) and Vertical Federated Learning (**VFL**) are roughly two fundamental categories of **FL**. In **HFL**, the system has common feature spaces in each regional dataset (parties may have their business market in the same domain) but distinct data samples. Conversely, sample spaces contain overlapping data samples in **VFL,** but they differ in data features. Two settings are derived from actual corporate situations in generating data, which in turn satisfy unique demands. Federated Transfer Learning (**FTL**) applies a unique direction and is suitable when the party's data is highly heterogeneous. In general, federated algorithms can be expanded according to how data is partitioned among clients and the basis nature of the data.

1.3 Technique Limitations and the objective of this work

Researchers have been improving the algorithmic mechanism for distributed learning over many computational sites in recent years.

In [8], the authors came up with a practical framework that help federated learning by model averaging. The results show a potential ability for adopting **FL** in other environments. However, the work left plenty of questions involving convergence guarantee and generalization performance. From the data perspective, the method further imposes the same amount of training workload with respect to each edge device, which raises uncertainty when deploying with actual data in unconventional domain. The algorithm also does not provide a clear and formal solution when tackling non-**IID** data, which is quite happened frequently.

FedProx [9] resolved mentioned cons thoroughly, and beyond that suggest a mathematical proof for their technique. They put up front a convergence analysis as well as local dissimilarity formulas for supporting convergence guarantee. The experiments showing the robustness under extremely heterogeneous setting are likewise presented. They allow some clients lazily perform fewer number of epochs and integrate a proximal term into local losses to penalizing the weights from being far away from the global model.

Nevertheless, almost all the state-of-the-art improvements mainly focus advancing security and statistical challenges. We realized an unhealthy assumption about hyperparameter selection, comes from the usages of canonical datasets. In this work, we simulate two algorithms **FedAvg** and **FedProx** two datasets which fit into two separate domains: (1) a brain tumor dataset with 3064 512×512 T1-weight images and (2) a VNPlant-200 dataset which includes 20,000 images of 200 unique medicinal plants. Firstly, we follow the stated process of training to obtain valuable observations, finding the optimal value for each hyperparameter. We adopt several **CNN**-based models like **VGG16**, **ResNet50, ConvNext, MaxViT** for comprehensive comparison. The number of communication rounds, i.e., the total communication cost until reaching a reasonable performance is our main metrics.

This work can be considered as a helpful reference for those who are interested in federated learning system or who currently being working with related fields.

2. RELATED WORKS

Many directions have significantly received attention during the decades. In the shape of federated optimization, the communication cost as well as the privacy effectiveness can be considered. Some works studied the statistical property of data, devices, and local gradients update.

In [10], iterative parameter mixing on structured perceptron is used to reduce the complexity given the availability the computing clusters. [11] utilize a format of elastic averaging: the asynchronous variant is also proposed. These works in general do not exam the non-**IID** nor the unbalance of datasets, which is a very principal for our upcoming settings. Remember that in a realistic scenario, the number of clients could be much larger than the number of data observations per client. In the convex setting,[12], [13] addressed some key concepts about federated framework: they particularly look at the privacy aspect during communicating, the upper and lower bound runtime and the quantity of used samples.

There are many publications that worked on minimizing communication cost [14], [15]. This approach decreases the overall runtime and jointly increases privacy performance. Opposed to iterative training approach, one endpoint of the distributed family is one-shot algorithm, which is the method that makes no overhead on communication cost at all. The final model is produced after all sub training processes finish, where in each sub process, a local client tries to solve the loss of its local data until reaching several epochs. The combine scheme could be model averaging. However, this method shows no better performance over minimizing on a single client [16], [17].

We have addressed earlier the importance of studying extensively the statistical property imposed on the nature of data and computing clusters. [18], [19] allow inexact local updating to balance computational cost and communication cost. This idea quite inspires for the systematic heterogeneity examination. Here we formalize some typical characteristics of federated learning problems: (1) local dataset will not be representative for the population distribution (non-**IID**), (2) unbalance data among devices, (3) the number of clients participating in learning could dominate the local dataset's size, (4) number of devices can be unavailable sometimes, (5) clients do not have the same computational strength, (6) updates could be lost during communication due to network issues.

We need to explore a more general framework that can handle heterogeneity introduced by characteristics mentioned above. The work in [20], [21]allowing data to be shared between clients and server for analyzing statistical feature lied in local data. This approach could help the server (or the coordinator) to inspect suitable solver use each round per client. Hence, the broader technique can be developed robustly to tackle highly non-**IID** and/or unbalanced dataset. Nonetheless, this puts a huge burden on network bandwidth (which is normally restricted in terms of hand-held devices or in case of non-physical connection). More seriously, the action of exchanging data violates the key aspect of privacy in a realistic federated environment: confidentiality.

One solution that comes naturally first in mind when dealing with device strength inequality is to abandon uncomplete training process or to use the result model weights regardless of a de-

vice finish its desired number of epochs or not. The same set of devices are likely to be exhausted more periodically all the time, thus, can bring bias to our model. Moreover, divergence could occur when profitable data in a particular device cannot maximize its productivity because of repudiation. [9] demonstrated that instability growths when we embrace some stragglers into chosen clients per round of communication. By adding proximal term to local loss function, [9]report several benefits in terms of communications cost and the stability of convergence. The randomized Kaczmarz method [22], [23] for solving linear systems of equations serves as an inspiration for the dissimilarity characterization analysis the authors offer.

Recent works adopting federated system in image tasks primarily use standard databases for experiments, such as **MNIST**, **CIFAR-10**, and their variations. This is advantageous because it expedites the experimentation of a vast number of parameter combinations, thereby facilitating the exploration and evaluation of more efficient algorithms. Few academics conduct federated learning on their domain-specific datasets. However, it has been observed that there is no established method of parameter optimization for dataset that is not specific to any domain. We would like to commence with utilizing the hyperparameter selection technique. Some key hyperparameters are: (1) the number of clients join in training each round, (2) the mini-batch size, (3) the number of epochs each round, (4) the μ hyperparameter of the proximal term, (5) the initial learning rate and rate decay algorithm. We wish to ascertain the influence of these parameters on new datasets to demonstrate the consistency of ultimate outcomes obtained at the end of the training procedure. Despite ensuring convergence, [9] still implies certain characteristics of [8], thus necessitating the requirement for an automated process for selecting parameters.

3. PROJECT MANAGEMENT PLAN

Table 1. Project Plan

Task name	Priority	Owner	Start date	End date	Status	Issues

Seek out research studies	High	K.L.H.	4/1/2023	29/1/2023	Completed	…
Setting up datasets	High	K.L.D.V.	4/1/2023	25/2/2023	Completed	…
Establish the FedAvg code environment.	High	K.L.H.	30/1/2023	15/2/2023	Completed	…
Establish the FedProx code environment.	High	K.L.H.	16/2/2023	15/3/2023	Completed	…
Run experiments on Brain Tumor Data	High	K.L.D.V.	16/2/2023	10/3/2023	Completed	…
Run experiments on VNPlant-200 datasets	High	K.L.D.V.	11/3/2023	10/4/2023	Completed	…
Review related papers for further improvements	Low	K.L.H.	16/3/2023	22/3/2023	Completed	…
Write report	High	K.L.H.	23/3/2023	10/4/2023	Completed	…
Revision	High	K.L.D.V. and K.L.H.	10/4/2023	17/4/2023	Completed	...

4. THEORETICAL FRAMEWORK

4.1 Stochastic Gradient Descent

SGD is commonly used as an optimization technique in contemporary works due to its ease of use. In addition, we cannot presume any bias at the beginning of the learning procedure; therefore, employing more complex algorithms could result in wasted effort without observing the actual effect of the FL setting.

SGD is an iterative method for optimizing an objective function by calculating the gradients for several samples, whereas GD utilizes the entire dataset to update the weights. Consider the scenario of minimizing the following loss function.

$$L(w) = \frac{1}{m}\sum_{i=1}^{m} L_i(w) \tag{1}$$

where w is the parameter being estimated and m is the number of data samples.

When using standard **GD**, an iteration of optimization strategy would be:

$$w \coloneqq w - \frac{\alpha}{m}\sum_{i=1}^{m} \nabla L_i(w) \tag{2}$$

Clearly, α is the learning rate. In classical statistics, this kind of sum-minimizing problem arises in least-squares (like linear regression) or in maximum-likelihood estimation. In simple form of loss objectives, step to global (or local) minimum is assured quickly. As a result of the intricacy of each local loss or the amount of the dataset, gradient calculation may be prohibitively costly in many situations. Performing each step on a subset of samples is preferable and is beneficial in large-scale **ML**.

$$w \coloneqq w - \alpha \nabla L_i \tag{3}$$

This time i represents the chosen training examples. The algorithms sweep through the entire dataset cause the loss functions to approach the optimum. The full process of learning by **SGD** for simple regression application can be roughly illustrated below.

Algorithm 1. Stochastic Gradient Descent

(1) Initialize weighs w and pick an initial learning rate α

(2) For each epoch (repeat until desired optimal value is achieved):

- Randomly shuffle data points in the dataset.
- For $i = 1,2,3,\dots,m$:
    - Determine the local loss $L_i = l(y - \hat{y})$

- $w \coloneqq w - \alpha \nabla L_i$

Given the capabilities of modern **GPUs** for parallel processing, the simple form of **SGD** is utilized infrequently due to its inefficient performance. The convergence of stochastic gradient descent has been widely investigated; particularly, given an acceptable learning rate, **SGD** will almost certainly cause the loss to reach its global minimum (convex case); otherwise, it will cause the loss to reach its local minimum.

Alternately, modifying the model's parameters now occurs in the form of a batch (called mini-batch stochastic gradient descent). The result of decreasing the mini-batch size could lead to more learning ability; said differently, this technique in fact allows the model converges faster than considering the whole dataset.

Algorithm 2. Mini-batch Stochastic Gradient Descent

(1) Initialize weighs w and pick an initial learning rate α

(2) For each epoch (repeat until desired optimal value is achieved):

a. Randomly shuffle data points in the dataset.

b. For each batch:

i. Determine the local loss $L = \sum_{i=1}^{b} l(y_i - \hat{y}_i)$

ii. $w \coloneqq w - \alpha \nabla L$

4.2 Federated Learning Algorithm

4.2.1 FedAvg Algorithm

FedAvg is built upon **SGD**, i.e., the local optimizer is typically **SGD**. In this subsection, we explore this approach in depth, formulate algorithms, and examine some of the original publication's results [8].

The combination of synchronous **SGD** (one partition must wait other partitions to finish computing gradients) and multi-batch updater yields best result. Consider *K* clients for whom

data is partitioned among, the hyper-parameter C controls the fraction of clients being chose per round. $C = 0$ means one client is chosen.

Each client k obtains $d_k = \nabla L_k(w_t)$ at completion of a training turn, then the server aggregates these gradients by:

$$w_{t+1} = w_t - \alpha \sum_{k=1}^{K} \frac{m_k}{m} d_k \tag{4}$$

where t denote the current communication round, and m_k represents the number of samples at client k.

The equivalent form can be achieved by alternating the derivatives at each local by its model's weights. This property is derived from:

$$w_{t+1}^k = w_t - \alpha d_k \tag{5}$$

$$w_{t+1} = \sum_{k=1}^{K} \frac{m_k}{m} w_{t+1}^k = w_t - \alpha \sum_{k=1}^{K} \frac{m_k}{m} d_k \tag{6}$$

One important design must be carefully considered when dealing with non-convex objectives. Independent initialization of a distributed model may result in poor performance. Averaging from different conditions shows no advantages over taking single evaluating in each model (the weight of mixing equals to 0 or 1). Conversely, when starting multiple models from a same random seed, averaging parameters works well.

Algorithm 3. FedAvg Algorithm

K is the number of clients. *C* is the fraction of clients selected per round. *B* is the local mini-batch size. *E* is the number of epochs each device must iterate through.

Server-side computation:

- initialize w_0
- for each round $t = 1,2,3, \ldots$
    - from *C*, select a random S_t subset from *K* clients

- for each client k in S_t
  - compute w_{t+1}^k by performing a client-side computation.
- $m_t \leftarrow \sum_{k \in S_t} n_k$ (The total number of data points involving into this training phase)
- $w_{t+1} \leftarrow \sum_{k \in S_t} \frac{m_k}{m_t} w_{t+1}^k$

Client-side computation:

- for each local epoch $i = 1,2,3, \dots, E$
  - for each batch b in the local dataset of this client
    - $w \leftarrow w - \alpha \nabla L(w, b)$
- return w_{t+1}^k

It is experimentally essential to properly tune the hyper parameter. *B* and *E* control the number of updates per round, which are quite similar in effectiveness. As previously indicated, in a federated system, communication costs are likely to outweigh computational costs, however in a centralized setting, communication costs are insignificant. In the meanwhile, C determines the global batch size, with the general assumption that in both **IID** and non-**IID** distributions, bigger C tends to reflect a larger proportion of data samples, resulting in better models for the current round. If we wish to add additional computing every round, we may either (1) increase parallelism (which has no negative effects if true parallelism is employed) or (2) increase computation at each client.

4.2.2 FedProx Algorithm

FedProx [9] can be perceived as a re-parameterization variant of **FedAvg** in which the authors introduce heterogeneous struggles. The study offers both empirical and theoretical investigations addressing the convergence of the approach.

As previously mentioned, more local computation can significantly help reduce communication costs. This amount is affected by the number of local epochs and the size of the local mini

batch. Besides that, more work of updating on each local landscape may cause each local model to converge toward its local optimum, hence, make convergence unpredictable. Some clients also cannot perform the desired number of updates due to hardware constraints. In practice, it is impossible to automatically determine in advance the suitable epoch for each client while the local epoch must satisfy the benefit of cutting communication cost. Therefore, to balance out the initial setting, **FedProx** fixes the number of epochs used for each round of communication and finds a more robust way to manage gradients received at the end. The proposed framework has two key characteristics.

Allow truncated work. Forcing all devices to implement the same effort of training is not quite realistic. **FedAvg** employs a basic approach: drop the uncomplete weights. This technique has been shown to produce bad models given a fixed number of rounds. The implementation specifies a new hyper parameter controls which clients completely participate in the result parameters and which does not. Inclusive experiments reveal the effectiveness of stability: throughout the learning procedure, loss tends to decrease consistency.

Proximal term. To prevent the weights from being far away from the global minimum, **FedProx** adjust the local solver to be more constrained:

$$L(w; w_0) = F(w) + \frac{\mu}{2}\|w_0 - w\|^2 \quad (7)$$

where $F(w)$ is the original distance with respect to local batch b and w_0 is the global weight at the beginning of the round. The additional term is beneficial both in: (1) overcome the heterogeneity in data distribution and (2) help for incorporating variable amounts of work from all clients.

Algorithm 4. FedProx Algorithm

K is the number of clients. C is the fraction of clients selected per round. B is the local mini-batch size. E is the number of epochs each device must iterate through. T is the number of stragglers.

Server-side computation:

- initialize w_0

- for each round $t = 1,2,3, \ldots$
    - from *C*, select a random S_t subset from *K* clients.
    - from *T*, select which client in S_t must perform full workload.
    - for each client *k* in S_t
        - compute w_{t+1}^k by performing a client-side computation (with assigned workload)
    - $m_t \leftarrow \sum_{k \in S_t} n_k$ (The total number of data points involving into this training phase)
    - $w_{t+1} \leftarrow \sum_{k \in S_t} \frac{m_k}{m_t} w_{t+1}^k$

Client-side computation:

- for each local epoch $i = 1,2,3, \ldots, E$
    - for each batch *b* in the local dataset of this client
        - $w \leftarrow w - \alpha \nabla L'(w, b)$, where $L'(w, b) = L(w, b) + \frac{\mu}{2} \|w_0 - w\|^2$
- return w_{t+1}^k

The optimizer is still stochastic gradient descent and fixed learning rate. Some works have been focused on employing other modern optimization algorithms as well as the automated manner to choosing learning rate.

4.3 Model's Architecture

In this section, we briefly introduce some architecture used in our experiments. The model decision is derived from related works in terms of commonly manipulating over used datasets.

4.3.1 VGGNet [24]

One remarkable exploration in this type of architecture is the adoption of a very deep **CNN** network combining with small receptive field. Particularly, 3 x 3 filters are used to replicate the effect of larger stride window while maintaining the reasonable size. This choice of design

shows a more accurate performance when we steadily append more convolutional layers to the model.

Generally, the family of architecture shares some settings:

- 224 x 224 RGB input image. The image is passed through a stack of conv layers with 3 x 3 filters.
- Stride is 1, same padding. That's why the very small receptive size is chosen: 3 x 3 is the smallest size that can capture the spatial information in the image.
- Five 2 x 2 max-pooling layers are used after some conv layers to reduce spatial dimension.
- Three fully connected layers at the end. The first two have 4096 units, while the last one's size depends on the label space's length.
- ReLU activation.

Detail configuration is showed in Table 2 below:

Table 2. VGGNet configuration

VGGNet Configuration					
VGG11	**VGG11-LRN***	**VGG13**	**VGG16**	**VGG16**	**VGG19**
224 x 224 RGB image					
conv3-64	conv3-64 LRN	conv3-64 conv3-64	conv3-64 conv3-64	conv3-64 conv3-64	conv3-64 conv3-64
maxpool					
conv3-128	conv3-128	conv3-128 conv3-128	conv3-128 conv3-128	conv3-128 conv3-128	conv3-128 conv3-128
maxpool					
conv3-256	conv3-256	conv3-256	conv3-256	conv3-256	conv3-256

conv3-256	conv3-256	conv3-256	conv3-256 conv1-256	conv3-256 conv3-256	conv3-256 conv3-256 conv3-256
maxpool					
conv3-512 conv3-512	conv3-512 conv3-512	conv3-512 conv3-512	conv3-512 conv3-512 conv1-512	conv3-512 conv3-512 conv3-512	conv3-512 conv3-512 conv3-512 conv3-512
maxpool					
conv3-512 conv3-512	conv3-512 conv3-512	conv3-512 conv3-512	conv3-512 conv3-512 conv1-512	conv3-512 conv3-512 conv3-512	conv3-512 conv3-512 conv3-512 conv3-512
maxpool					
FC-4096					
FC-4096					
FC-L**					
softmax layer					

Note that: (*) **LRN** stands for local responses normalization and (**) represents the number of labels in the label space.

4.3.2 ResNet [25]

ResNet leverages the neural network's depth to a higher level. Stacking more layers makes it difficult to train due to vanishing/exploding gradients. Simply put, this issue can be addressed

by adding normalization. However, the result tends to degradation while training loss does not guarantee to be decreased, i.e., overfit is not the case. This phenomenon indicates that there is a problem with deep layer that makes it harder to learn more fine-grained features, which is the key principle in deep learning. **ResNet** introduces residual blocks to cope with this dilemma.

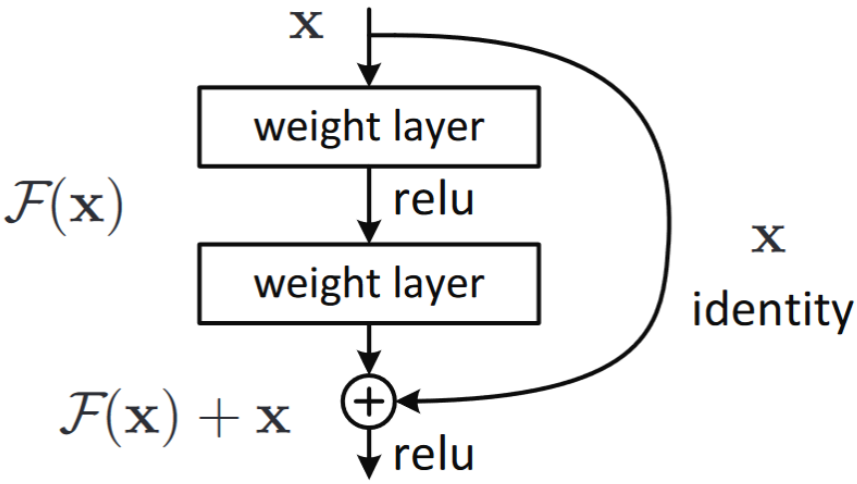

Figure 2. Residual Block (image from original paper [25])

The identity short-connection quantity helps to optimize the desired function easier because now if the eventual performance of the identity mapping is optimum, learning process just needs to push residual term to zero.

Comprehensive experiments on ImageNet [26] showed that: (1) deeper networks indeed result higher accuracy and (2) networks with residual block are easier to train compared to plain counterpart. Table 3 lists the structure of different depth **ResNet**.

Table 3. ResNet's architecture (L denotes the label space length, square brackets denote residual blocks)

layer type	18-layer	34-layer	50-layer	101-layer	152-layer
conv	7 x 7, 64 channels, stride 2				
conv	$\begin{bmatrix} 3\times 3, 64 \\ 3\times 3, 64 \end{bmatrix} \times 2$	$\begin{bmatrix} 3\times 3, 64 \\ 3\times 3, 64 \end{bmatrix} \times 3$	$\begin{bmatrix} 1\times 1, 64 \\ 3\times 3, 64 \\ 1\times 1, 256 \end{bmatrix} \times 3$	$\begin{bmatrix} 1\times 1, 64 \\ 3\times 3, 64 \\ 1\times 1, 256 \end{bmatrix} \times 3$	$\begin{bmatrix} 1\times 1, 64 \\ 3\times 3, 64 \\ 1\times 1, 256 \end{bmatrix} \times 3$

conv	$\begin{bmatrix}3\times3,128\\3\times3,128\end{bmatrix}\times2$	$\begin{bmatrix}3\times3,128\\3\times3,128\end{bmatrix}\times4$	$\begin{bmatrix}1\times1,128\\3\times3,128\\1\times1,512\end{bmatrix}\times4$	$\begin{bmatrix}1\times1,128\\3\times3,128\\1\times1,512\end{bmatrix}\times4$	$\begin{bmatrix}1\times1,128\\3\times3,128\\1\times1,512\end{bmatrix}\times8$
conv	$\begin{bmatrix}3\times3,256\\3\times3,256\end{bmatrix}\times2$	$\begin{bmatrix}3\times3,256\\3\times3,256\end{bmatrix}\times6$	$\begin{bmatrix}1\times1,256\\3\times3,256\\1\times1,1024\end{bmatrix}\times6$	$\begin{bmatrix}1\times1,256\\3\times3,256\\1\times1,1024\end{bmatrix}\times23$	$\begin{bmatrix}1\times1,256\\3\times3,256\\1\times1,1024\end{bmatrix}\times36$
conv	$\begin{bmatrix}3\times3,512\\3\times3,512\end{bmatrix}\times2$	$\begin{bmatrix}3\times3,512\\3\times3,512\end{bmatrix}\times3$	$\begin{bmatrix}1\times1,512\\3\times3,512\\1\times1,2048\end{bmatrix}\times3$	$\begin{bmatrix}1\times1,512\\3\times3,512\\1\times1,2048\end{bmatrix}\times3$	$\begin{bmatrix}1\times1,512\\3\times3,512\\1\times1,2048\end{bmatrix}\times3$
pool-ing	avgpooling				
fully con-nected	L-dim fc				
activa-tion	softmax layer				

4.3.3 ConvNext [27]

As the introduction of Vision Transformers (**ViT**) in 2020, the computer vision landscape is not limited to network architecture design. **ViT** surprisingly show potential results on image classification tasks given the ability to scaling. Nonetheless, computer vision also contains other difficult duties involving in image-specific inductive bias to maximize spatial information. Without ConvNet, a vanilla **ViT** model may confront a few challenges in dealing with object detection or semantic segmentation.

Many advancements have been made to bring back ConvNet to form a hybrid approach [28]. The sliding window method shows their role as being intrinsic to visual processing. However, these works have some costly components, which could cause the design to be more complex

or be unreasonable to scale. **ConvNext**, a pure ConvNet model is built gradually by embracing some minor design modifications. This process aims to mimic the way a hybrid transformer model like Swin Transformer [28] process digital images.

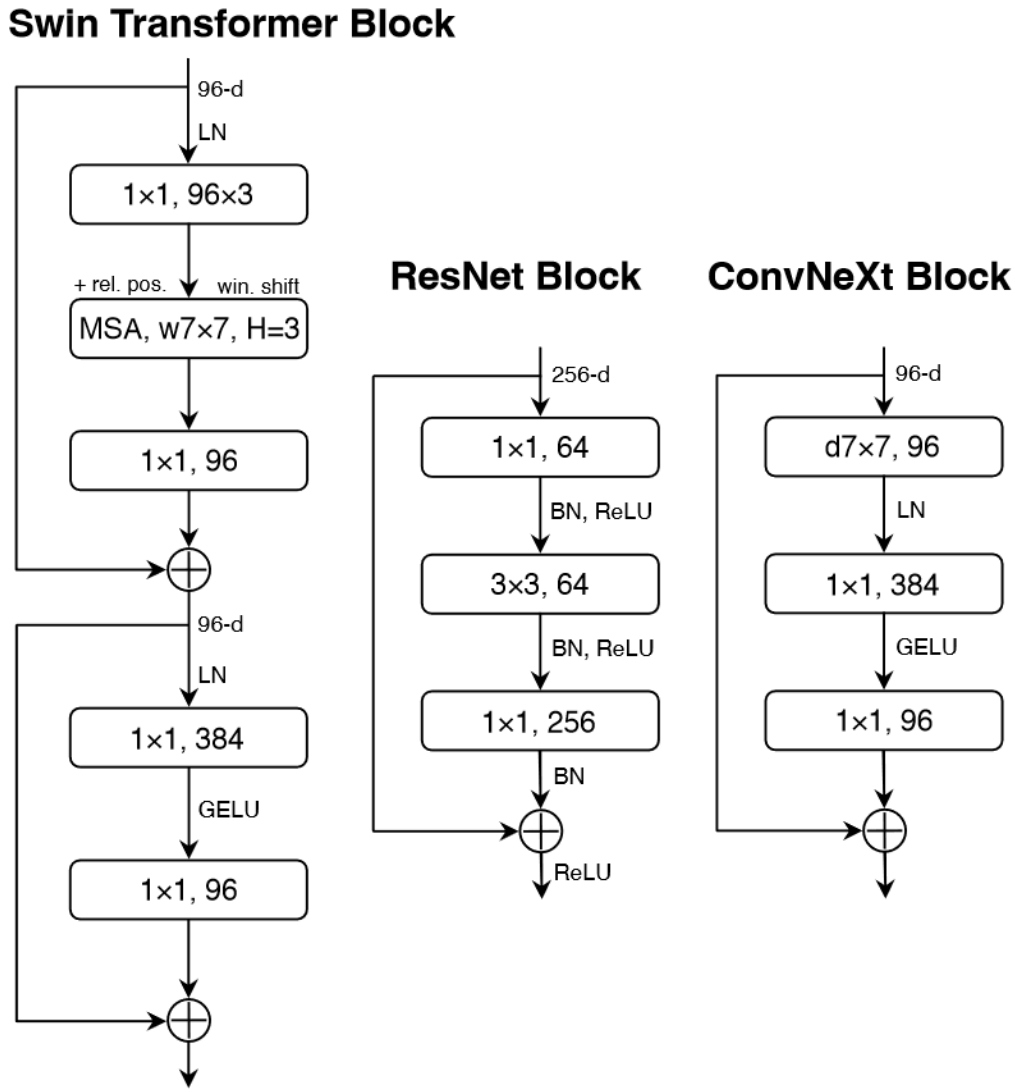

Figure 3. Comparison of a basis block design in **Swin Transformer**, **ResNet** and **ConvNext** (image from original paper [27])

Training Technique. Increase the number of epochs from 90 to 300. **AdamW** Optimizer is adopted. Various augmentation techniques like Mixup, CutMix, RandAugment, RandomErasing. Stochastic Depth and Label Smoothing are used for regularization.

ResNext-ify. Depthwise Convolution is used to group convolution filters.

Inverted Bottleneck. The idea is that we could adopt inverted bottleneck in **ResNet**. The hidden dimension within a layer block is now 4 times bigger than input dimension.

Large Kernel Size. To examine the behavior of large size kernel, **ConvNext** moves up the position of the depthwise conv layer. (However, this violates a typical standard of using small receptive field to replicate the effect of larger kernel size to gain parallel computing of modern GPU). **ConvNext** also experiment also kernel size include 3, 5, 7, 9, 11. The performance saturates when the number reaches 7.

Micro Design. ReLU is replaced by GELU. Some activation positions are also eliminated. Truncate batch normalization and some are altered with layer normalization. Separate downsampling layers.

4.3.4 MaxViT [29]

Added multi-axis attention helps form an efficient attention model to cope with scalability. There are two novel ideas in this work: blocked local and dilated global attention. The proposed model called **MaxViT** serves as a powerful vision backbone for visual processing.

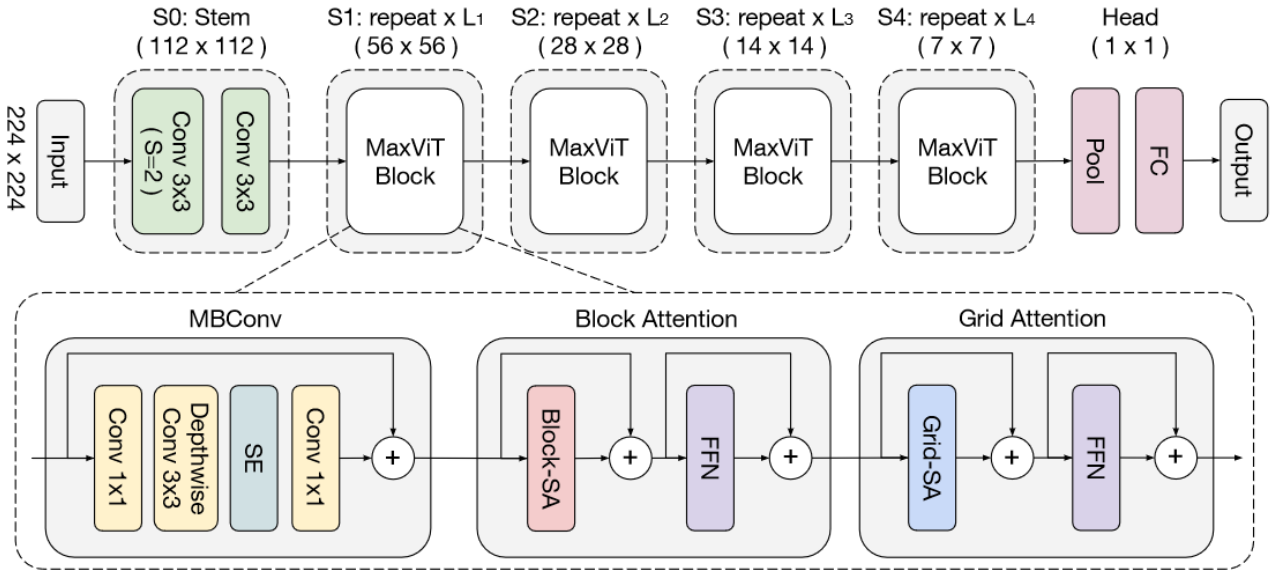

Figure 4. **MaxViT** architecture (image from original paper [29])

5. MATERIALS AND METHODS

5.1 Resources

All presented works in the scope of this report are performed on Google Collaboratory Pro+. Hardware specifications vary over time. Typical details are:

Table 4. Hardware specs

	Standard	**Premium**
CPU	Intel(R) Xeon(R) CPU @ 2.20 GHz	Intel(R) Xeon(R) CPU @ 2.20 GHz
RAM	12 GB	84 GB
GPU	NVIDIA Tesla T4 16 GB VRAM	NVIDIA A100 40 GB VRAM

5.2 Datasets and Implementation Details

We use the brain tumor dataset composed by Cheng et al. [30] in the first class of experiments. The dataset consists of 3064 T1-weighted pictures collected from 233 patients with three labels of brain malignancies: 708 images of meningioma, 1426 images of glioma, and 930 images of pituitary tumor. Figure 5 illustrates some sample images taken in [30]. The images have digital resolution of 512×512 with pixel size of 0.49×0.49 mm^2.

We split the datasets into 80% training and 20% test. Test set is resided at the aggregation server, while training samples are partitioned into 10 clients. Partition manners are discussed later. For image pre-processing, Contrast Limited Adaptive Histogram Equalization (**CLAHE**) technique is adopted. The image is then resized to 224×224.

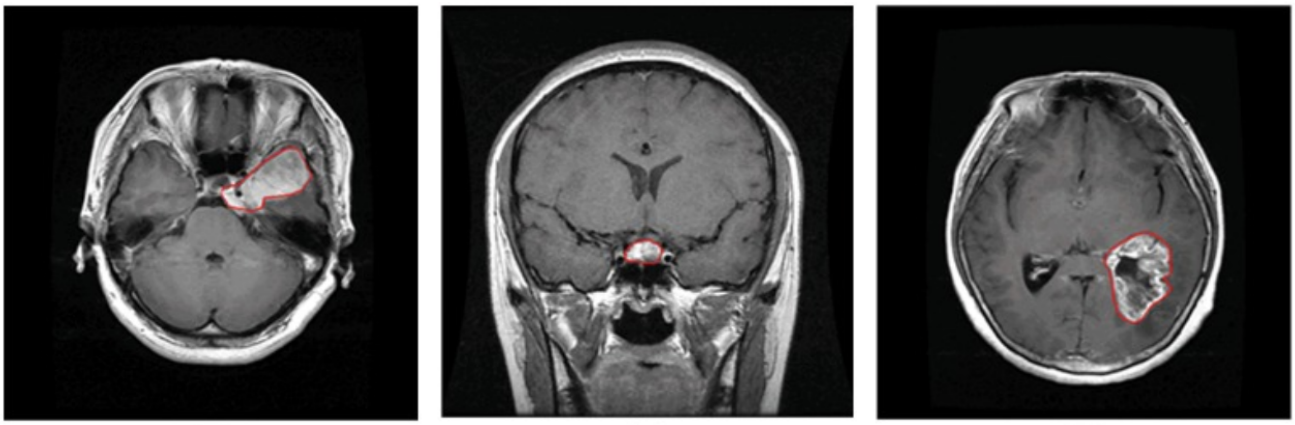

(a) **(b)** **(c)**

Figure 5. Three types of brain tumor: (a) meningioma; (b) glioma; and (c) pituitary tumor.

With second class of experiment, an herbal plant dataset which consists of plants found in Vietnam are used. The photographs were captured within a natural setting with the intention of depicting the intricacy of classifying images within real world environments. The dataset comprises of plant images captured from varying angles, brightness levels, environmental conditions, viewpoints, and other related factors. Thus, it serves as a suitable model for a practical plant recognition task. Figure 6 demonstrates some samples.

Figure 6. VNPlant-200 sample images.

After resizing to 224 × 224, we implement some data augmentation like random rotation or random flip. We use 8000 images for testing, 2000 images for validation, and the rest for training. This time the number of devices jointly learning the federated model is 100.

Table 5. VNPlant-200 characteristics

Number of species	200
Number of images for each specie	100
Image resolution	256 × 256 and 512 × 512
Angle	Entire plant with realistic noise
Environment	Real world

Data distribution approach. To study federated performance on heterogeneity setting, we explore two ways to partition data. In **IID** way, the data is randomly shuffled and distributed over *K* clients, i.e., each client theoretically represents the whole population. Non-**IID** manner involves sorting the data points by labels first, then populate each client with an equal number of samples so that each client contains at most 2 labels. This way we could benchmark both algorithms on specific domain non-**IID** data for generalization.

Regarding learning rates used in **SGD**, we tune for the best value achieved by each combination of hyper parameters, i.e., all numbers shown in tables or figures are training on the best learning rate. One critical point: for fair competition, we fix the randomly selected clients, the order of mini batch per client across training rounds. We also apply plain **FedAvg** algorithm while dropping the testing of stragglers in **FedProx**. That means we do not incorporate variable works on those devices, instead we force all chose devices to perform the same amount of work.

6. RESULTS and DISCUSSION

6.1 Brain Tumor classification task

6.1.1 Comprehensive summarization on FedAvg scheme

Partial parallelism. We first play with client fraction *C*. Table 6 shows the results of varying *C* over Brain tumor dataset. **VGG16** is used as the initial baseline. We adopt a slightly different methodology here: instead of evaluating the cost of communication until satisfying desired levels of accuracy, we record the test-set accuracy obtained when finishing given numbers of rounds. Here, the approach functions effectively in an **IID** setting that provides positive outcomes with just small communication rounds. Undoubtedly, greater C produces better outcomes, particularly in non-**IID** settings when client data do not reflect the whole distribution. The performance of non-IID data improves with time more slowly than **IID** data, indicating that communication cost is substantial in non-**IID** scenarios. Comparing our results to those of the original study, in which the authors conducted tests on **MNIST** using two basic neural networks, we detect a comparable impact. Table A1 in the appendix section illustrates this effect in the original paper. Figure A1, A2 in the appendix section gives a clearer view regarding the speed of convergence over rounds of communication.

Table 6. Impact of varying *C* on the Brain tumor dataset using **FedAvg** algorithm on **VGG16** model. $E = 5, B = 10$. Each entry represents the test-set accuracy received at given rounds of communication.

C	**IID**				**Non-IID**			
	10	20	50	100	10	20	50	100
0.1	92.48	95.26	97.38	98.20	47.39	47.39	63.40	72.22
0.2	94.12	96.41	98.04	98.53	47.39	79.08	87.09	90.69
0.3	95.26	96.24	97.55	98.37	77.29	77.29	91.12	94.12
0.5	95.45	97.55	98.04	98.20	83.49	88.56	93.62	95.59

For consistent insights and balance out the computational weight of training due to limited hardware constraints, we fix $\boldsymbol{C = 0.2}$ for further testing.

Local computation examination. This time, the influence of extra local computation is investigated. Adding extra updates every round to each client does not significantly increase performance. We attempt to raise E from 1 to 5, while altering the mini-batch size to the values 4, 10, and 16. Nonetheless, we discover a very intriguing property: a mini-batch size of 16 yields a pretty good result in a non-**IID** context. In some instances, the performance suffers when the mini batch size is increased while the number of epochs is maintained, indicating that too many updates might lead averaging to give inferior results. The counterpart diagram of Table 7 is placed at Figure A3, A4 at appendix, in which we visualize the effect we have done here.

Table 7. Various cases when device's amount of update is altered. Model is **VGG16**. $\boldsymbol{C = 0.2}$

E	B	IID				Non-IID			
		10	20	50	100	10	20	50	100
1	10	86.11	93.30	96.08	96.57	55.72	55.72	79.08	89.38
2	10	93.46	94.93	97.55	98.37	66.01	66.67	80.39	90.69
5	4	95.26	96.70	98.04	98.04	55.88	77.94	87.58	90.85
5	10	94.12	96.41	98.04	98.53	47.39	79.08	87.09	90.69
5	16	93.95	96.41	97.71	97.88	67.32	67.32	80.23	93.30

So far, the documented experiments have demonstrated a reliable set of hyper parameter values for our task. We study further the impact of several classifiers on federated learning. Comparing **ResNet50**, **ConvNext**, and **MaxViT** with the **VGG16** baseline, we employ several cutting-edge deep learning architectures. Table 8 displays the experimental states. In this series of studies, E=5, B=16, and C=0.2 are used for non-IID data whereas E=5, B=10, and C=0.2 are used for IID data.

Table 8. Comparison of some state-of-the-art deep learning models with federated learning on Brain Tumor dataset. E=5, B=16, and C=0.2 for non-IID data and E=5, B=10, and C= 0.2 for IID data.

	IID				**Non-IID**			
Rounds of com.	10	20	50	100	10	20	50	100
VGG16	94.12	96.41	98.04	98.53	67.32	67.32	80.23	93.30
ConvNext	95.52	96.57	98.04	98.69	75.65	75.65	80.88	92.16
ResNet50	91.83	95.59	96.73	98.03	49.51	71.24	82.52	86.76
MaxVit	94.93	96.57	97.56	98.69	56.86	75.82	85.95	90.36

Evidently, **ConvNext** and **MaxViT** give superior outcomes while processing IID data. On the other hand, despite the fact that ConvNext is the best model during the first 50 rounds of communications, it cannot exceed the peak performance of **VGG16**. Consequently, **VGG16**, with 93,3% accuracy, may be the best reliable classifier for non-IID Brain Tumor image data. Figure A5, A6 in the appendix provides more visualization details.

6.1.2 Comprehensive summarization on FedProx scheme

Following the preceding section's work, we examine if the proximal term in FedProx aids in handling non-**IID** situations. We have found that B=16 and E=5 produce decent results in non-**IID** contexts, thus we will continue to use these parameters in the subsequent tests. **ConvNext** and **VGG16**, which produced the greatest results on the Brain Tumor dataset in the previous section, are also reused. In this effort, we tweak the $\boldsymbol{\mu}$ hyper parameter from a limited candidate set of $\{\mathbf{0}, \mathbf{0.001}, \mathbf{0.01}, \mathbf{0.1}, \mathbf{1}\}$ to determine its effect on test-set accuracy convergence after 10, 20, 50, and 100 rounds of communications. Tables 9 and 10 show the respective outcomes of **ConvNext** and **VGG16**.

Table 9. Test-set accuracies of **FedProx** federated algorithm with various $\boldsymbol{\mu}$ on Brain Tumor dataset. The classifier is **ConvNext**, B=16, E=5.

μ	Non-IID			
	10	20	50	100
0	75.65	75.65	80.88	92.16
1	79.08	79.08	85.29	92.48
0.1	80.23	80.23	83.82	92.65
0.01	76.31	76.31	83.99	92.65
0.001	78.59	78.59	86.11	92.48

Table 10. Test-set accuracies of **FedProx** federated algorithm with various μ on Brain Tumor dataset. The classifier is **VGG16**, B=16, E=5.

μ	Non-IID			
	10	20	50	100
0	67.32	67.32	80.23	93.30
1	60.94	62.58	83.33	93.30
0.1	48.04	72.06	83.01	89.05
0.01	60.29	67.97	83.17	91.83
0.001	71.90	80.39	80.39	81.21

We can see that, given an appropriate value of μ, the learning process tends to be condensed into fewer iterations and assured to converge steadily over time. With **ConvNext**, the optimal value of μ is 0.1, allowing the accuracy to surpass 80% in only 10 communication rounds. In case of **VGG16**, the optimal value of μ for fast convergence is 0.001. With **VGG16**, however, there is a little trade-off: the faster convergence comes at the expense of a lower peak accuracy, in this instance 81.21% as opposed to 93.3%. This conduct has no impact on **ConvNext**.

The heterogeneity breaking behavior of **FedProx** over **FedAvg** will be described in the next section. However, we would like to stress a vital point: it is essential to choose a suitable number for μ; otherwise, the performance might decrease and become unstable over time.

6.1.3 Heterogeneity advantages study on FedProx

In figure 7, we see that **FedProx** yields quite humble results compared to **FedAvg**. Although the convergence property is assured, it does not seem reliable in terms of stability, early conver-

gence, or peak performance. The candidate set of proximal term parameter μ taken from original work. Here we can conclude that the disparity tackling effect of **FedProx** is not remarkable.

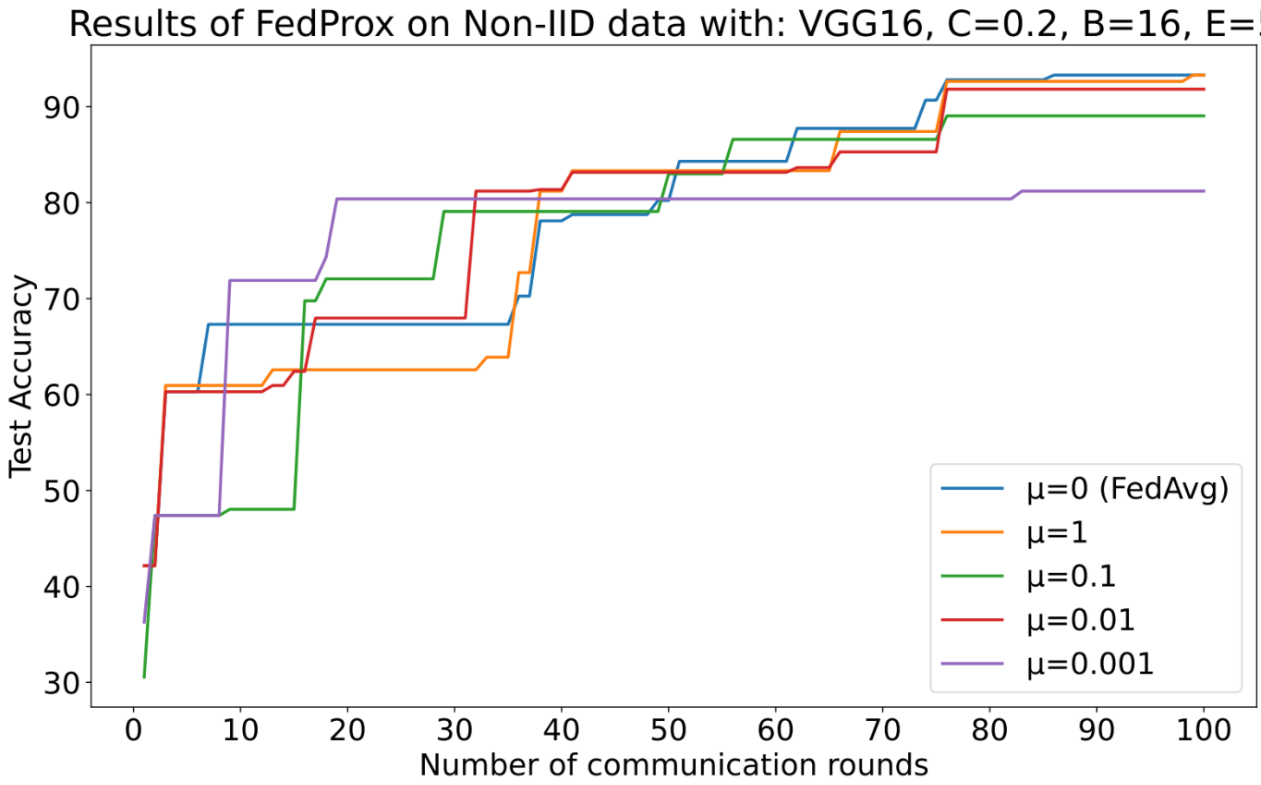

Figure 7. Results comparison between **FedAvg** and **FedProx** with various μ values on **Brain Tumor** dataset. (**ConvNext**)

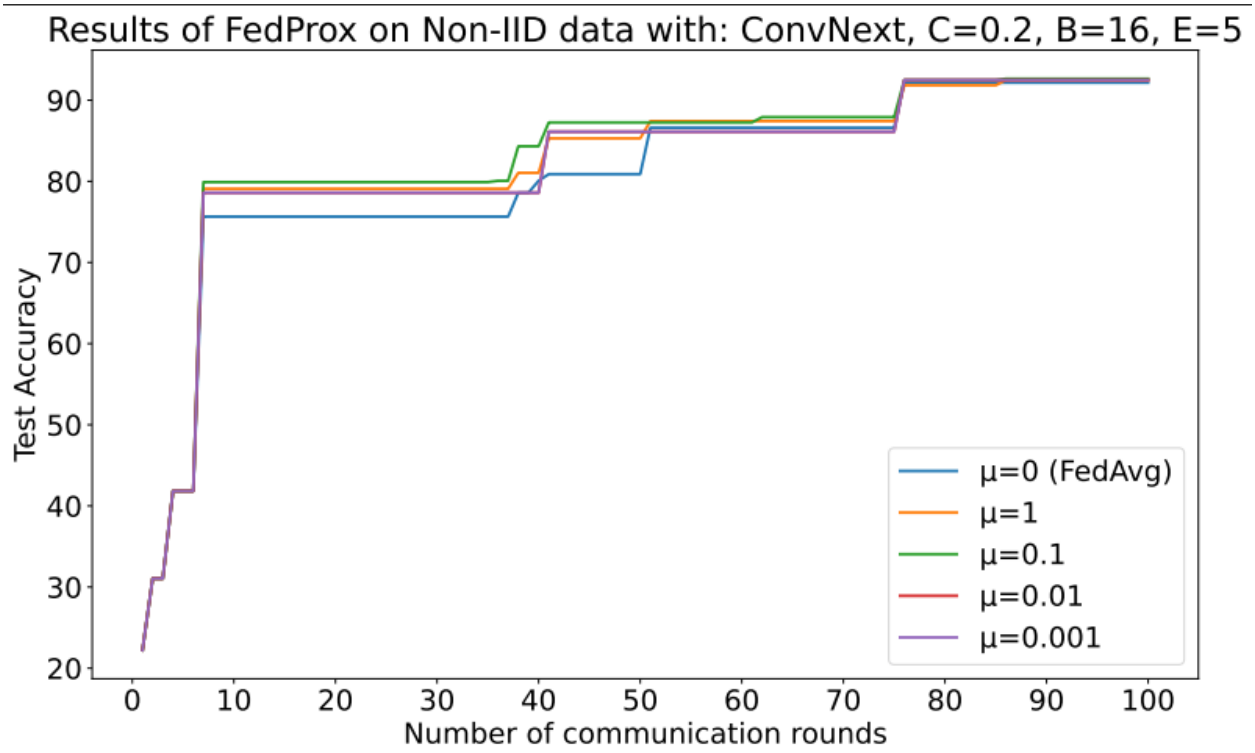

Figure 8. Results comparison between **FedAvg** and **FedProx** with various μ values on **Brain Tumor** dataset. (**VGG16**)

6.2 Medicinal Plant classification task

We follow the same methodology of model evaluation here. The conclusions are quite like those obtained above, so we will only stress important points as we progress our experiments.

6.2.1 Comprehensive summarization on FedAvg scheme

Table 11. Impact of varying C on the **VNPlant-200** dataset using **FedAvg** algorithm on **VGG16** model. $E = 5, B = 10$. Each entry represents the test-set accuracy received at given rounds of communication.

C	IID				Non-IID			
	10	20	50	100	10	20	50	100
0.1	68.34	77.84	84.95	85.56	10.44	12.81	20.00	31.80
0.2	77.08	82.90	86.80	88.56	33.39	41.35	60.19	67.81
0.3	80.34	85.15	88.04	89.24	38.13	53.61	70.65	74.68
0.5	81.71	86.76	89.09	89.09	51.73	66.40	77.71	81.28

In this family of experiments in Table 11, we could see large differences in performance regarding both data distribution case or the cardinality of clients per round. This observation can be derived from the fact that the harder identification task is involved. We see $C = 0.1$ produce poor results on non-**IID** setting and increase C extremely mitigating this problem. Convergence speed analysis can be conducted here. Figure A7, A8 show more illustrative insights.

Table 12. Different local computational imposed on each client per round under $C = 0.2$ using **VGG16** model. **FedAvg** is used. **VNPlant-200** is under investigation.

E	B	IID				Non-IID			
		10	20	50	100	10	20	50	100
5	10	77.08	82.9	86.8	88.56	33.39	41.35	60.19	67.81
5	16	78.48	83.41	87.59	88.93	31.61	41.59	58.60	68.76
5	32	79.38	84.13	86.69	88.28	31.51	44.14	57.39	66.66
1	10	55.60	70.00	81.20	85.71	21.49	36.04	48.56	63.11
2	10	65.03	78.36	84.75	88.64	26.96	38.33	58.53	67.34

Again, in Table 12, we see there are no significant differences between those cases. This implies the stated arguments in the original paper are not universal. Hence, putting effort in tuning this kind of parameter needs to be studied more extensively. Table 13 experiments model choice effect. Other intuitive plots are resided in appendix, Figure A9, A10, A11, A12.

Table 13. The effect of various classifiers regarding the **VNPlant-200** dataset. **FedAvg** is the algorithm. The mini batch size, the number of local epochs, the client fraction are 16, 5, and 0.2, respectively.

Model	IID				Non-IID			
	10	20	50	100	10	20	50	100
VGG16	78.48	83.41	87.59	88.93	31.61	41.59	58.6	68.76
ConvNext	86.40	91.29	93.59	94.51	30.86	48.15	68.11	73.09
ResNet50	82.73	87.93	91.94	93.10	34.51	48.15	72.85	82.65
MaxVit	79.41	88.64	92.65	94.01	36.76	43.08	69.79	76.33

6.2.2 Comprehensive summarization on FedProx scheme

Follow up previous sections, we conduct similar operations with the same observations on **FedProx** technique over **VNPlant-200** dataset. Since **ResNet50** brings best results on former experiments, we keep using this deep network on current class of expriments. Mini batch size is 16, and number of local epochs is 5 (since dozens of our works reveal that the variant in terms of the amount of local update does not impact so much on the ultimate performance). Again, we tune the proximal term weight from predefined set of candidates. The results is showed in Table 14.

Table 14. Experiments upon the weight of proximal quantity on **VNPlant-200** dataset. $\boldsymbol{B = 16, E = 5, C = 0.2}$. The classifier is ResNet50.

μ	Non-IID			
	10	20	50	100
0	34.51	48.15	72.85	82.65
1	35.48	50.00	73.23	82.95
0.1	34.76	48.48	73.13	82.37
0.01	34.34	50.93	73.10	82.71
0.001	35.24	49.60	73.81	82.41

As we can see, the numbers are quite clear. Adding more constrain into the local losses tends to slightly increase our test-set accuracy. We have not tested with larger μ, but in the publised paper, the authors indicates that huge μ would cause the learning process to be very low.

6.2.3 Heterogeneity advantages study on FedProx

The visualization of Table 14 is shown in Figure 8. The improvement is quite small, but it is still there. Futher inspectation is required to understand the behavior of this hyper parameter. However, adding the proximal term will always guarantee convergence, as proven by the approach's authors.

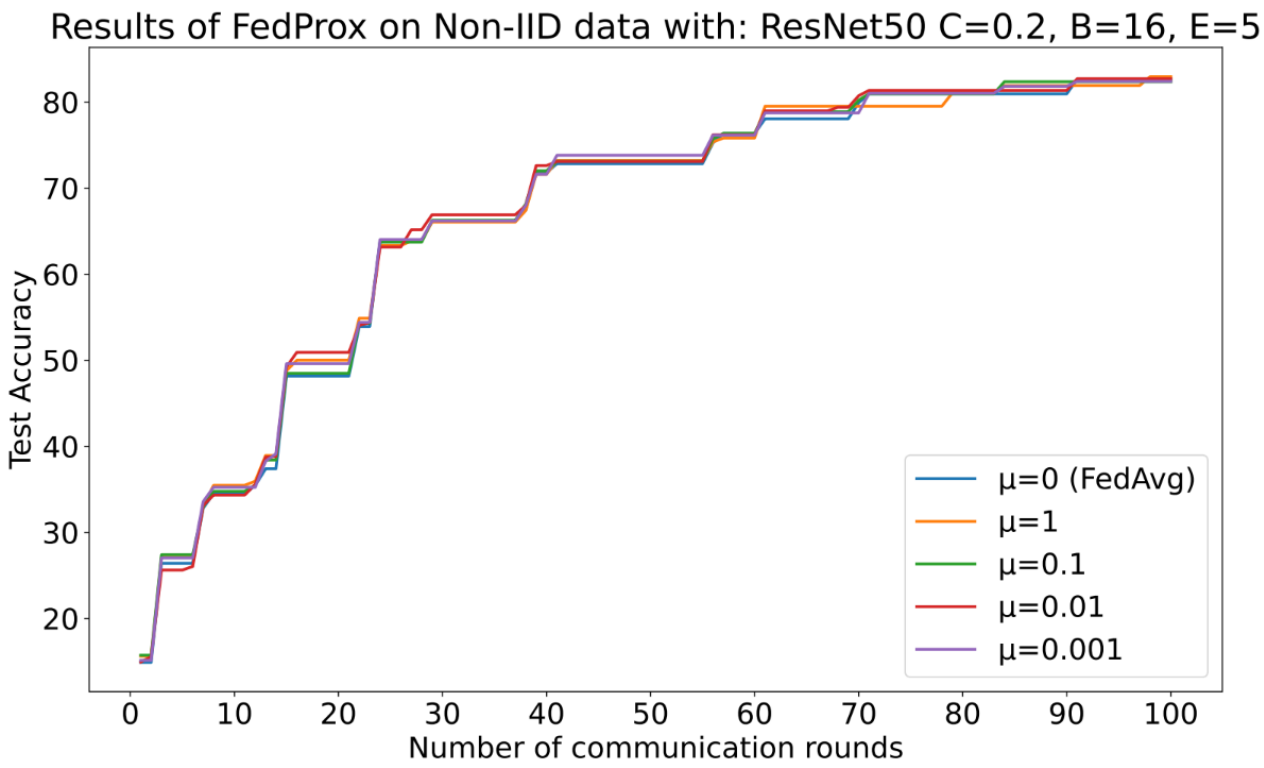

Figure 9. Results comparison between **FedAvg** and **FedProx** with various μ values in **VNPlant-200** dataset.

7. CONCLUSIONS AND PERSPECTIVES

Federated Learning is truly a novel and intriguing approach for data scientists. Its approach is both similar and different from other decentralized learning methods that have appeared before: the burden of communication costs must be considered, and some effort is required in encoding to ensure data privacy and integrity. If this optimization is done well, we can efficiently leverage the abundant data sources worldwide from end-users, especially as data privacy laws are increasingly tightened and the artificial intelligence industry is reaching saturation due to the lack of increased data sources as before.

In this work, we employed two federated learning methods, **FedAvg** and **FedProx**, on two datasets to examine their efficacy. We tuned the parameters based on the guidance provided in the original paper. Each dataset was split into two portions: a training set and a test set. The training set was distributed among a set of clients, while the test set was used by the server to

evaluate the results. We utilized simple preprocessing and data augmentation techniques to test the experimental viability of federated learning. Two data allocation methods were employed: **IID** and non-**IID**. The classifiers utilized in this study were well-known and classic deep learning models. We derived the following conclusions:

(1) The averaging of model parameters is truly effective, especially in the case of **IID**. In the case of non-**IID**, the results are also promising, even without any significant data augmentation methods and only using simple optimization methods.

(2) The higher the number of clients participating in each round of communication, the higher the model performance. Of course, ensuring accuracy at the beginning of each round depends on practical conditions, network connectivity, and device availability. However, in general, the more data coming from different sources each round allows the model to converge closer to the optimal point.

(3) Adjusting the local update quantity per client per round does not significantly improve performance. As long as this update quantity balances computational and communication costs and is not updated excessively in one round, the model's convergence is ensured.

(4) The choice of classifier for each problem depends on relevant studies and the nature of the problem and data, rather than the federated learning method itself. Of course, the model must be selected to be suitable for the hardware capabilities and data quantity at each client.

(5) Non-**IID** remains a significant challenge: experiments consistently show a sharp decline in accuracy in the non-**IID** setting, and even converge to a saturation point of average accuracy despite increasing rounds of communication. **FedProx** seems to fall short of achieving the maximum attainable accuracy that can be compared to the **IID** setting (and even worse than the centralized training setting). Nevertheless, FedProx with appropriate parameters still provides a slight improvement. One thing to clarify is that we did not apply the approach of discarding clients that cannot complete the assigned training task. It is possible that we will integrate this in future studies.

(6) Federated Learning results can vary significantly when the difficulty level of the task changes, and the impact of hyperparameters also varies accordingly. However, there is still a safe range for the parameters that determine the computation load per round at each client. As for the trend of the client fraction parameter, it remains unchanged.

We have observed a significant aspect worth investigating: defining the parameters of the optimization solver. More advanced methods such as **RMSProp**, **GD** with momentum, and **AdamW** can be used. Learning rate decay can also be considered.

CONFLICTS OF INTEREST: The authors declare no conflict of interest.

8. REFERENCES

[1] S. Pouyanfar *et al.*, "A Survey on Deep Learning," *ACM Comput Surv*, vol. 51, no. 5, pp. 1–36, Sep. 2019, doi: 10.1145/3234150.

[2] W. G. Hatcher and W. Yu, "A Survey of Deep Learning: Platforms, Applications and Emerging Research Trends," *IEEE Access*, vol. 6, pp. 24411–24432, 2018, doi: 10.1109/ACCESS.2018.2830661.

[3] J. Deng, J. Guo, N. Xue, and S. Zafeiriou, "ArcFace: Additive Angular Margin Loss for Deep Face Recognition," in *2019 IEEE/CVF Conference on Computer Vision and Pattern Recognition (CVPR)*, IEEE, Jun. 2019, pp. 4685–4694. doi: 10.1109/CVPR.2019.00482.

[4] J. Guo, J. Deng, A. Lattas, and S. Zafeiriou, "SAMPLE AND COMPUTATION REDISTRIBUTION FOR EFFICIENT FACE DETECTION," in *ICLR 2022 - 10th International Conference on Learning Representations*, 2022.

[5] I. Kemelmacher-Shlizerman, S. M. Seitz, D. Miller, and E. Brossard, "The MegaFace benchmark: 1 million faces for recognition at scale," in *Proceedings of the IEEE Computer Society Conference on Computer Vision and Pattern Recognition*, 2016. doi: 10.1109/CVPR.2016.527.

[6] A. Nech and I. Kemelmacher-Shlizerman, "Level playing field for million scale face recognition," in *Proceedings - 30th IEEE Conference on Computer Vision and Pattern Recognition, CVPR 2017*, 2017. doi: 10.1109/CVPR.2017.363.

[7] S. Yang, P. Luo, C. C. Loy, and X. Tang, "WIDER FACE: A face detection benchmark," in *Proceedings of the IEEE Computer Society Conference on Computer Vision and Pattern Recognition*, 2016. doi: 10.1109/CVPR.2016.596.

[8] H. Brendan McMahan, E. Moore, D. Ramage, S. Hampson, and B. Agüera y Arcas, "Communication-efficient learning of deep networks from decentralized data," in *Proceedings of the 20th International Conference on Artificial Intelligence and Statistics, AISTATS 2017*, 2017.

[9] T. Li, A. K. Sahu, M. Zaheer, M. Sanjabi, A. Talwalkar, and V. Smith, "FEDERATED OPTIMIZATION IN HETEROGENEOUS NETWORKS Tian," *MLSys*, 2020.

[10] R. McDonald, K. Hall, and G. Mann, "Distributed training strategies for the structured perceptron," in *NAACL HLT 2010 - Human Language Technologies: The 2010 Annual Conference of the North American Chapter of the Association for Computational Linguistics, Proceedings of the Main Conference*, 2010.

[11] S. Zhang, A. Choromanska, and Y. Lecun, "Deep learning with elastic averaging SGD," in *Advances in Neural Information Processing Systems*, 2015.

[12] M. F. Balcan, A. Blum, S. Fine, and Y. Mansour, "Distributed learning, communication complexity and privacy," in *Journal of Machine Learning Research*, 2012.

[13] O. Shamir and N. Srebro, "Distributed stochastic optimization and learning," in *2014 52nd Annual Allerton Conference on Communication, Control, and Computing, Allerton 2014*, 2014. doi: 10.1109/ALLERTON.2014.7028543.

[14] Y. Zhang, J. C. Duchi, M. I. Jordan, and M. J. Wainwright, "Information-theoretic lower bounds for distributed statistical estimation with communication constraints," in *Advances in Neural Information Processing Systems*, 2013.

[15] O. Shamir, N. Srebro, and T. Zhang, "Communication-efficient distributed optimization using an approximate Newton-type method," in *31st International Conference on Machine Learning, ICML 2014*, 2014.

[16] Y. Zhang, J. C. Duchi, and M. J. Wainwright, "Communication-efficient algorithms for statistical optimization," *Journal of Machine Learning Research*, vol. 14, 2013.

[17] Y. Arjevani and O. Shamir, "Communication complexity of distributed convex learning and optimization," in *Advances in Neural Information Processing Systems*, 2015.

[18] S. Boyd, N. Parikh, E. Chu, B. Peleato, and J. Eckstein, "Distributed optimization and statistical learning via the alternating direction method of multipliers," *Foundations and Trends in Machine Learning*, vol. 3, no. 1. 2010. doi: 10.1561/2200000016.

[19] O. Dekel, R. Gilad-Bachrach, O. Shamir, and L. Xiao, "Optimal distributed online prediction using mini-batches," *Journal of Machine Learning Research*, vol. 13, 2012.

[20] Eunjeong Jeong, Seungeun Oh, Hyesung Kim, Jihong Park, Mehdi Bennis, and Seong-Lyun Kim, "Communication-Efficient On-Device Machine Learning: Federated Distillation and Augmentation under Non-IID Private Data".

[21] Y. Zhao, M. Li, L. Lai, N. Suda, D. Civin, and V. Chandra, "Federated learning with non-iid data," *arXiv*. 2018.

[22] S. KACZMARZ, "Approximate solution of systems of linear equations†," *Int J Control*, vol. 57, no. 6, 1993, doi: 10.1080/00207179308934446.

[23] T. Strohmer and R. Vershynin, "A randomized kaczmarz algorithm with exponential convergence," *Journal of Fourier Analysis and Applications*, vol. 15, no. 2, 2009, doi: 10.1007/s00041-008-9030-4.

[24] K. Simonyan and A. Zisserman, "Very deep convolutional networks for large-scale image recognition," in *3rd International Conference on Learning Representations, ICLR 2015 - Conference Track Proceedings*, 2015.

[25] K. He, X. Zhang, S. Ren, and J. Sun, "Deep residual learning for image recognition," in *Proceedings of the IEEE Computer Society Conference on Computer Vision and Pattern Recognition*, 2016. doi: 10.1109/CVPR.2016.90.

[26] O. Russakovsky *et al.*, "ImageNet Large Scale Visual Recognition Challenge," *Int J Comput Vis*, vol. 115, no. 3, 2015, doi: 10.1007/s11263-015-0816-y.

[27] Z. Liu, H. Mao, C. Y. Wu, C. Feichtenhofer, T. Darrell, and S. Xie, "A ConvNet for the 2020s," in *Proceedings of the IEEE Computer Society Conference on Computer Vision and Pattern Recognition*, 2022. doi: 10.1109/CVPR52688.2022.01167.

[28] Z. Liu *et al.*, "Swin Transformer: Hierarchical Vision Transformer using Shifted Windows," in *Proceedings of the IEEE International Conference on Computer Vision*, 2021. doi: 10.1109/ICCV48922.2021.00986.

[29] Z. Tu *et al.*, "MaxViT: Multi-axis Vision Transformer," in *Lecture Notes in Computer Science (including subseries Lecture Notes in Artificial Intelligence and Lecture Notes in Bioinformatics)*, 2022. doi: 10.1007/978-3-031-20053-3_27.

[30] J. Cheng *et al.*, "Enhanced performance of brain tumor classification via tumor region augmentation and partition," *PLoS One*, vol. 10, no. 10, 2015, doi: 10.1371/journal.pone.0140381.

9. Appendix

Before starting this section, we are glad to announce that our work on this report has been accepted by IEEE **Zooming Innovation in Consumer Technologies International Conference** (**ZINC**) 2023, a place for both industry and academic field. The conference is included in the **ZINC** 2023 events, which is sponsored by IEEE Serbia and Montenegro Section – Consumer Technology Chapter; the University of Novi Sad, Faculty of Technical Sciences, Computer Engineering and Computer Communications Group and RT-RK Institute for Computer-Based Systems. For more information, please visit: https://www.gozinc.org/ . Below are the accept email from the organizing committee and our first-version draft of our paper.

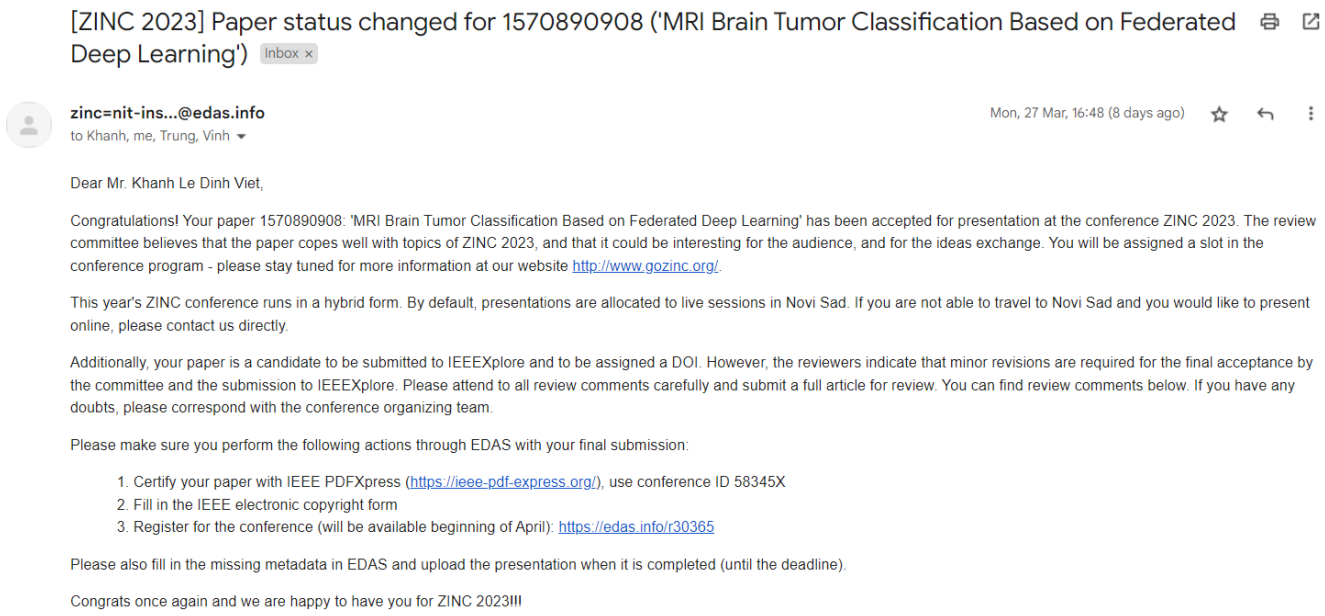

[ZINC 2023] Paper status changed for 1570890908 ('MRI Brain Tumor Classification Based on Federated Deep Learning') Inbox ×

zinc=nit-ins...@edas.info Mon, 27 Mar, 16:48 (8 days ago)
to Khanh, me, Trung, Vinh

Dear Mr. Khanh Le Dinh Viet,

Congratulations! Your paper 1570890908: 'MRI Brain Tumor Classification Based on Federated Deep Learning' has been accepted for presentation at the conference ZINC 2023. The review committee believes that the paper copes well with topics of ZINC 2023, and that it could be interesting for the audience, and for the ideas exchange. You will be assigned a slot in the conference program - please stay tuned for more information at our website http://www.gozinc.org/.

This year's ZINC conference runs in a hybrid form. By default, presentations are allocated to live sessions in Novi Sad. If you are not able to travel to Novi Sad and you would like to present online, please contact us directly.

Additionally, your paper is a candidate to be submitted to IEEEXplore and to be assigned a DOI. However, the reviewers indicate that minor revisions are required for the final acceptance by the committee and the submission to IEEEXplore. Please attend to all review comments carefully and submit a full article for review. You can find review comments below. If you have any doubts, please correspond with the conference organizing team.

Please make sure you perform the following actions through EDAS with your final submission:

1. Certify your paper with IEEE PDFXpress (https://ieee-pdf-express.org/), use conference ID 58345X
2. Fill in the IEEE electronic copyright form
3. Register for the conference (will be available beginning of April): https://edas.info/r30365

Please also fill in the missing metadata in EDAS and upload the presentation when it is completed (until the deadline).

Congrats once again and we are happy to have you for ZINC 2023!!!

MRI Brain Tumor Classification based on Federated Deep Learning

Khanh Le Dinh Viet*, Khiem Le Ha*, Trung Nguyen Quoc*, Vinh Truong Hoang†
*Department of Information Technology, FPT University, Ho Chi Minh city, Vietnam
{khanhldvse150118, khiemlhse150198, trungnq46}@fpt.edu.vn
†Faculty of Information Technology
Ho Chi Minh City Open University, Vietnam
vinh.th@ou.edu.vn

***Abstract*—The proliferation of artificial intelligence (AI) has the potential to revolutionize many industries, but its application is hindered by the shortage of large-scale data. Data in various domains often exist in isolated silos, necessitating privacy and security. In the meantime, the lack of access to medical privacy prevented the development of trustworthy systems for diagnosing deadly malignancies like brain tumors. In this study, we apply a federated learning algorithm known as Federated Averaging (FedAvg) to train a brain tumor classification system using decentralized data without requesting the exchange of sensitive data. The proposed framework's hyperparameters are adjusted to enhance its effectiveness on both independently and identically (IID) and non-independently and identically distributed data (Non-IID). Additionally, we leverage four cutting-edge deep learning models, namely, VGG16, ResNet50, ConvNeXt, and MaxViT, to optimize classification accuracy. The proposed framework achieves a classification accuracy of 98.69% on IID data and over 93% on Non-IID data.**

***Index Terms*—Federated learning; VGG16; ResNet50; ConvNeXt; MaxViT; Brain Tumor**

I. Introduction

Artificial intelligence (AI) systems' supremacy has recently been demonstrated by their robust applications across practically all industries, including object detection, face recognition, and recommendation systems, etc [1]. More complex machine learning (ML) models as well as the availability of a large amount of data are supporting this rapid expansion. The most crucial element in the future era of this technology is anticipated to be big data-driven in order to disseminate the effects of AI [2]. However, data only exists in the form of isolated islands, making it expensive to transfer enough data to build trustworthy AI models. Additionally, data leaks are occasionally impossible due to privacy and security concerns in a number of specific businesses, like banking and the medical field. As a result, the most likely way to implement AI applications in the actual world is no longer data centralization. Federated learning was proposed [3] as a technique to handle isolated data islands without any requests for data transmission or leakage. Federated learning, in overview, is a training technique that enables to guide models based on data that is distributed across multiple devices or data centers without the need to transfer data to a central location [2]. This method has shown promise in addressing privacy and scalability issues in real-world AI applications, particularly in the medical industry.

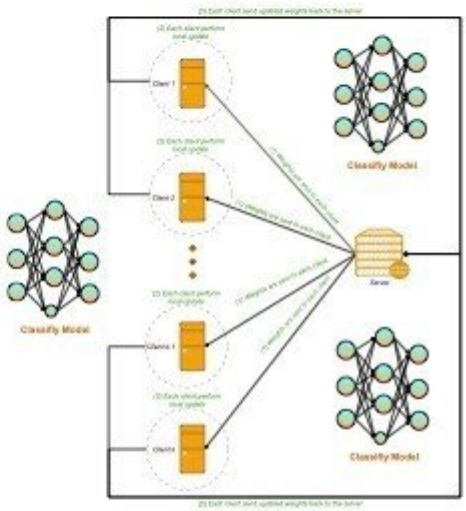

Fig. 1: The illustration of Federated learning system.

Some dangerous illnesses, such as brain malignancies, which can drastically reduce life expectancy, are nevertheless discovered by manual diagnostic imaging. Due to their reliance on radiologists' expertise, these conventional practices could have a number of drawbacks. Therefore, integrating deep learning models into computer-aided diagnosis (CAD) systems will inevitably become popular in order to increase the accuracy of diagnoses made using medical pictures. However, because patient information is private, it seems impossible to gather enough image samples to create a trustworthy diagnosis system. In these situations, using a decentralized training method like federated learning could be a great way to handle the issues.

In this project, a federated learning algorithm called as FedAvg [4] is applied to some state-of-the-art deep learning frameworks to conduct a brain tumor classification system without the need of centralizing data samples. The following are the primary contributions of this study

- The dataset is distributed to ten clients to simulate the way that data is organized in the industry.
- Fine-tuning the federated learning algorithm to figure out the most suitable hyperparameters for use with a specific brain tumor dataset.
- Integrating cutting-edge deep learning architectures into the classification framework and measuring their effectiveness.

The remainder of this article is organized as follows: In Section II, we discuss relevant prior work in the field. Section II describes the organization of the dataset and the approach used in this study. The results of our experiments are then presented in Section IV, while Section V concludes the paper.

II. Related Works

In recent years, there has been a growing interest in the use of federated learning for various medical applications, owing to its advantages in preserving the privacy of isolated data. One of the earliest use of federated learning in medicine is the study of Sheller et al. [5], who demonstrated the effectiveness of federated learning in the task of brain tumor segmentation. In their strategy, numerous institutions worked together to train a common deep neural network, where each client provided its own patient data without revealing it to others. Although achieves high performance, Sheller's framework relies on a central server, which could result in an unstable and unreliable system. In order to deal with this issue, Roy et al. [6] suggest an alternative federated learning algorithm known as BrainTorrent to deploy the training process in a peer-to-peer manner. The performance of this framework proved to be better than the traditional server-based method on a similar problem of brain tumor segmentation. In 2021, chest CT images from seven global clinical centers were gathered by Qi Dou et al [7] to assess the viability of a federated learning system for COVID-19 illness detection. According to the study's conclusions, federated learning might be a useful technique for quickly creating CAD systems across organizations and nations to counter the pandemic without having to worry about sensitive information becoming out to the public.

A unique data-driven strategy to automatically aggregate model weights based on data distributions across the training process was recently developed by Xia Y. et al. [8]. The authors then went on to show how well this technique worked when it came to segmenting COVID-19 lesions in chest CT and pancreas in abdominal CT. When working with unknown samples, Tian C. X. et al. [9] employed a specific gradient alignment loss to maintain the model stable throughout training. The authors also set up some tests to demonstrate the viability of the suggested framework in two different medical image classification tasks.

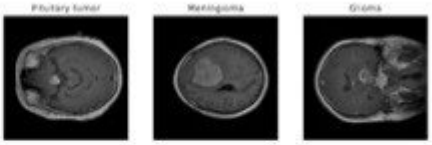

Fig. 2: Three types of brain tumor.

III. Methods

A. Data Preparation

In this study, the dataset [10], which consists of 3064 MRI T1-weight brain tumor images, is used to demonstrate the effectiveness of the federated learning algorithm for classifying medical images. Figure 2 shows an illustration of each brain tumor type. This original data then was split into training set and testing set followed by the ratio of 8:2, respectively. In order to simulate the isolated form of data in the real world, the sample images of three types of brain tumors in training set, namely, meningioma, glioma, and pituitary tumor, are randomly distributed into 10 independent clients. However, the data from a particular client sometimes might not represent the identified distribution of the global data, which causes statistical heterogeneity challenges to prevent the convergence of the classification model. Thus, the dataset is additionally distributed to clients as a non independently and identically distributed version (Non-IID) by sorting the labels of medical images, instead of a sequence of naive randoms.

B. The Classification Framework

The classification framework used for training decentralized data commonly includes two key factors. The first one is the classifier model for categorizing input images, while the second one is the aggregation algorithm for synthesizing the best global model parameter from local information. In this work, 4 cutting-edge deep learning-based designs such as VGG16 [11], ResNet50 [12], ConvNeXt [13], and MaxViT [14], are integrated into the federated learning to figure out their classification performance in an isolated data situation of the medical industry.

Meanwhile, FedAvg, a federated learning technique proposed by Google [4], is adapted to aggregate useful information for the central classifier model. In the deployment of FedAvg, at each communication round, a fraction of total clients (C) is permitted to prioritize optimizing the local model based on a given batch size (B) and a number of epochs (E). After receiving the updated local weights of communicated clients, the central server applies a simple mechanism of averaging these weights and then loading them for the global

C	IID				Non-IID			
	10	20	50	100	10	20	50	100
0.1	92.48	95.26	97.38	98.20	47.39	47.39	63.4	72.22
0.2	94.12	96.41	98.04	98.53	47.39	79.08	87.09	90.69
0.3	95.26	96.24	97.55	98.37	77.29	77.29	91.12	94.12
0.5	95.45	97.55	98.04	98.20	83.49	88.56	93.62	95.59

TABLE I: Baseline results with VGG16, batch size $B = 10$, and number of epochs $E = 5$.

E	B	IID				Non-IID			
		10	20	50	100	10	20	50	100
5	10	94.12	96.41	98.04	98.53	47.39	79.08	87.09	90.69
5	16	93.95	96.41	97.71	97.88	67.32	67.32	80.23	93.30
1	10	86.11	93.30	96.08	96.57	55.72	55.72	79.08	89.38
2	10	93.46	94.93	97.55	98.37	66.01	66.67	80.39	90.69
5	4	95.26	96.70	98.04	98.04	55.88	77.94	87.58	90.85

TABLE II: Model performance when fixing $C = 0.2$, and changing B and E.

model. Finally, these new parameters will be synchronized for all of the clients in the system, and then a new communication round could be started again. Figure 1 demonstrate the design of the studied framework.

IV. Experimental Results

In order to optimize the classification accuracy after a fixed number of communication rounds, many experiments are organized to figure out the optimal hyperparameter as well as the best classifier model for this brain tumor dataset. All of the experiments are implemented and run on Google Colab Pro Plus, which consumes more than 600 computing units equivalent to 300 hours of training. The federated learning algorithm is conducted by Python scripts without the support from any federated learning frameworks.

The baseline results firstly are conducted by choosing VGG16 as the classifier, a batch size of 10, and $E = 5$. The outcomes, which are shown in Table I, prove that increasing the number of clients trained in each round surely leads to the improvement of the final performance. Additionally, when dealing with then Non-IID data, the system with a small value of C might suffer to achieve convergence. Due to the clear idea that a high number of clients helps to achieve high accuracy, the rest experiments in this study would fix the value of C as 0.2 for reducing the burden of computing, and finding the optimal value of another hyperparameter such as a number of epochs E or batch size B. Table II presents how E and B could affect to the training results of the federated learning framework. When increasing the value of B from 10 to 16, the best accuracy on IID data at a particular communication round is significantly reduced, while that change helps robust the accuracy on Non-IID data from 90.69% to 93.30%. That improvement proves that a batch size of 16 might be more effective in the process of dealing with Non-IID data. Meanwhile, the batch size of 4 also is employed for the experiment but could not make any remarkable enhancements. For the adjustment of the number of epochs, $E = 1$ and $E = 2$ are further applied to the training system, while keeping all of the other hyperparameters. However, similar to the case of a batch size of 4, these adjusted results still could not overcome the previous results with $E = 5$.

Model	IID				Non-IID			
	10	20	50	100	10	20	50	100
VGG16	94.12	96.41	98.04	98.53	67.32	67.32	80.23	93.30
ConvNeXt	95.52	96.57	98.04	98.69	77.29	78.43	87.41	92.16
ResNet50	91.83	95.59	96.73	98.03	49.51	71.24	82.52	86.76
MaxViT	94.93	96.57	97.56	98.69	56.86	75.82	85.95	90.36

TABLE III: The comparison of some state-of-the-art deep learning models with the brain tumor dataset

So far, the experiments are shown in Table I and Table II already figured out the optimal configuration for handling both IID data and Non-IID data. The study further fine-tunes the classification system by evaluating more state-of-the-art deep learning designs, namely, ResNet50, ConvNeXt, and MaxViT. The results of these works are presented in Table III. Compared with the baseline model of VGG16, the best accuracy of ConvNeXt and MaxViT architectures at particular communication rounds significantly outperform the original results on IID data. After 100 rounds, ConvNeXt would be the best model for handling the task of brain tumor classification when dealing with IID data, with 98.69% accuracy. With Non-IID data, although the best accuracy of ConvNeXt is better than VGG16 after first 50 rounds, it still cannot overcome the peak of VGG16 when ending up the training process of 100 rounds. Thus, VGG16, with 93.30% accuracy, might be the most possible classifer to tackle Non-IID data.

V. Conclusions

For the purpose of developing a brain tumor classification system without centralizing data samples, the efficacy of a federated learning algorithm known as FedAvg is being examined in this study. As a simulation of industrial forms, the dataset is disseminated to 10 clients in two different methods (IID and Non-IID). Based on that, the system's hyperapameters are modified to improve classification accuracy. Thus, the federated learning system with ConvNeXt as the classifier achieves remarkable performance on classifying three types of brain tumors, with 98.69% accuracy on IID data, while the one of VGG16 peaks at 93.30% accuracy on Non-IID data. The difficulties associated with statistic heterogeneity as non-independent and indivisible data, however, have not yet been fully resolved, making the convergence process unstable and susceptible to "unseen" data. As a result, there is greater room for this federated learning system to be improved by more effectively addressing the problems with Non-IID data.

References

[1] Samira Pouyanfar, Saad Sadiq, Yilin Yan, Haiman Tian, Yudong Tao, Maria Presa Reyes, Mei-Ling Shyu, Shu-Ching Chen, and S. S. Iyengar. A survey on deep learning. *ACM Computing Surveys*, 51:1–36, 9 2019.

[2] Qiang Yang, Yang Liu, Tianjian Chen, and Yongxin Tong. Federated machine learning. *ACM Transactions on Intelligent Systems and Technology*, 10:1–19, 3 2019.

[3] Jakub Konečný, H. Brendan McMahan, Daniel Ramage, and Peter Richtárik. Federated optimization: Distributed machine learning for on-device intelligence. 10 2016.

[4] H. Brendan McMahan, Eider Moore, Daniel Ramage, Seth Hampson, and Blaise Agüera y Arcas. Communication-efficient learning of deep networks from decentralized data. 2 2016.

[5] Micah J. Sheller, G. Anthony Reina, Brandon Edwards, Jason Martin, and Spyridon Bakas. Multi-institutional deep learning modeling without sharing patient data: A feasibility study on brain tumor segmentation. pages 92–104, 2019.

[6] Abhijit Guha Roy, Shayan Siddiqui, Sebastian Pölsterl, Nassir Navab, and Christian Wachinger. Braintorrent: A peer-to-peer environment for decentralized federated learning. 5 2019.

[7] Qi Dou, Tiffany Y. So, Meirui Jiang, Quande Liu, Varut Vardhanabhuti, Georgios Kaissis, Zeju Li, Weixin Si, Heather H. C. Lee, Kevin Yu, Zuxin Feng, Li Dong, Egon Burian, Friederike Jungmann, Rickmer Braren, Marcus Makowski, Bernhard Kainz, Daniel Rueckert, Ben Glocker, Simon C. H. Yu, and Pheng Ann Heng. Federated deep learning for detecting covid-19 lung abnormalities in ct: a privacy-preserving multinational validation study. *npj Digital Medicine*, 4:60, 3 2021.

[8] Yingda Xia, Dong Yang, Wenqi Li, Andriy Myronenko, Daguang Xu, Hirofumi Obinata, Hitoshi Mori, Peng An, Stephanie Harmon, Evrim Turkbey, Baris Turkbey, Bradford Wood, Francesca Patella, Elvira Stellato, Gianpaolo Carrafiello, Anna Ierardi, Alan Yuille, and Holger Roth. Auto-fedavg: Learnable federated averaging for multi-institutional medical image segmentation. 4 2021.

[9] Chris Xing Tian, Haoliang Li, Yufei Wang, and Shiqi Wang. Privacy-preserving constrained domain generalization for medical image classification. 5 2021.

[10] Jun Cheng, Wei Huang, Shuangliang Cao, Ru Yang, Wei Yang, Zhaoqiang Yun, Zhijian Wang, and Qianjin Feng. Enhanced performance of brain tumor classification via tumor region augmentation and partition. *PLOS ONE*, 10:e0140381, 10 2015.

[11] Karen Simonyan and Andrew Zisserman. Very deep convolutional networks for large-scale image recognition. 9 2014.

[12] Kaiming He, Xiangyu Zhang, Shaoqing Ren, and Jian Sun. Deep residual learning for image recognition. 12 2015.

[13] Zhuang Liu, Hanzi Mao, Chao-Yuan Wu, Christoph Feichtenhofer, Trevor Darrell, and Saining Xie. A convnet for the 2020s. pages 11966–11976. IEEE, 6 2022.

[14] Zhengzhong Tu, Hossein Talebi, Han Zhang, Feng Yang, Peyman Milanfar, Alan Bovik, and Yinxiao Li. Maxvit: Multi-axis vision transformer. 4 2022.

We also conduct to write another paper to sumit at **Information Systems International Conference** (**ISICO**) 2023. This event is held by **Department of Information Systems, Institut Teknologi Sepuluh Nopember** (**ITS**). The seventh **ISICO** 2023 title is "Breakthrough Information Systems Innovations Toward Digital Resilience, Reinvention, and Transformation". This year, the conference is in a hybrid plafform: held virtually and on-site (Prama Sanur Beach) in Sanur, Bali, Indonesia on 26-28 July, 2023. For more information, please visit: https://isico.info

Available online at www.sciencedirect.com

ScienceDirect

Procedia Computer Science 00 (2023) 000–000

Procedia Computer Science

www.elsevier.com/locate/procedia

Seventh Information Systems International Conference (ISICO 2023)

Medicinal Plants Identification Using Federated Deep Learning

Khanh Le Dinh Viet[a], Khiem Le Ha[a], Trung Nguyen Quoc[a], Vinh Truong Hoang[b]

[a]*Department of Information Technology, FPT University, Ho Chi Minh city, Vietnam*
[b]*Faculty of Information Technology, Ho Chi Minh City Open University, Vietnam*

Abstract

Over the years, scientists have discovered bioactive chemicals in many of the plants that have been traditionally utilized as medicinal medicines. However, identifying plant species based on their physical characteristics can be difficult, and misidentification can have severe consequences, such as the use of the incorrect plant as a medicine. With the advent of machine learning techniques such as deep learning and federated learning, it is now possible to develop automated systems for the precise image-based classification of medicinal plants. Nevertheless, medicinal plant classification using deep learning techniques typically requires a large amount of data, which can be challenging to acquire and manage due to privacy concerns, data ownership, and geographic reasons. Federated learning provides a solution to this issue by enabling the training of a shared model on multiple devices without requiring centralized data storage. In this work, we assess and optimize the federared learning framework using two federated learning approaches, FedAvg and FedProx, and four state-of-the-art deep learning networks for the job of categorizing medicinal plants by distributing the original training set into two forms, IID and Non-IID. Ultimately, the accuracy of the optimal federated learning system is improved by 5.65% and 14.84% over the baseline on IID data and Non-IID data, respectively. Furthermore, the study brings up a new difficult arena for the task of classifying medicinal plants using Non-IID training data.

Keywords: Medicinal Plants; Federated Learning; Classification; Deep Learning

1. Introduction

Since ancient times, medicinal plants have been utilized to treat a wide range of ailments and diseases. Although the use of medicinal plants has decreased as modern medicine has developed, their significance in traditional and alternative medicine has not diminished. The identification and use of medicinal plants in traditional medicine, as well as their preservation and protection in the wild, depend on their classification. However, manual observation and study of plant traits used in conventional methods of classification can be time-consuming and prone to inaccuracy.

The accuracy and speed of medicinal plant classification have recently showed significant promise thanks to recent developments in machine learning, particularly deep learning. However, the availability and caliber of training data have a significant impact on how well machine learning models perform. Given that these plants are frequently found in secluded and difficult-to-reach places, gathering big and diverse datasets for the classification of medicinal plants can be a considerable difficulty.

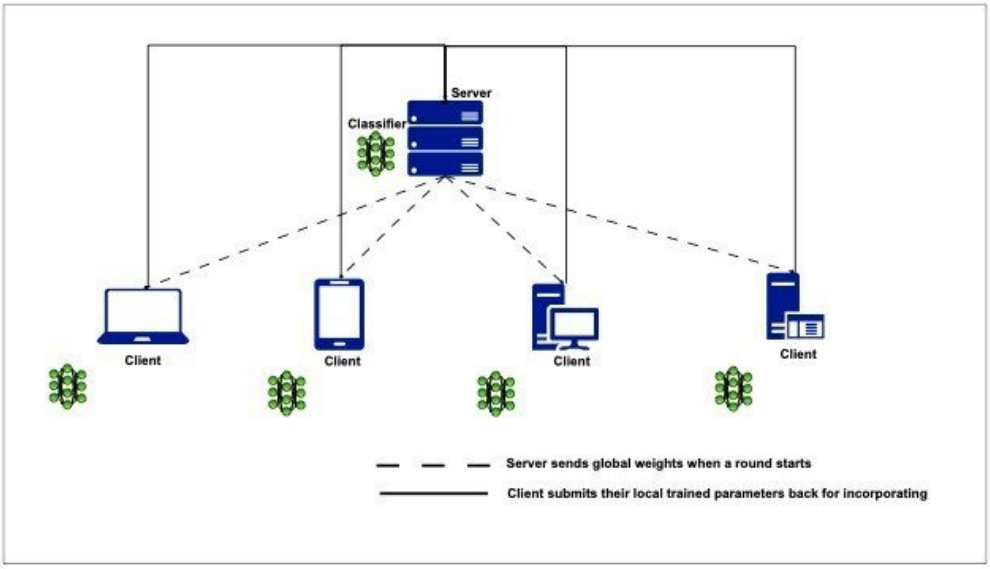

Fig. 1: The illustration of federated learning system.

A new machine learning paradigm called federated learning [21] tackles the difficulties associated with training models on distributed and decentralized data. Without sharing their data with a central server, several clients, each with their own dataset, work together to build a shared machine learning model in federated learning. This method provides various benefits, including higher scalability, improved data privacy, and less communication expenses.

In this study, we investigate the use of federated learning in the identification of medicinal plants. By utilizing two federated learning algorithms, FedAvg [10] and FedProx [7], we specifically study the efficacy of federated learning in training deep learning models on decentralized and distributed datasets of medicinal plant photos. In a restricted number of communication rounds, we also assess the effects of several model architectures and hyper-parameters on the accuracy of classification results and compare how well federated learning performs on two data distribution methodologies.

The remainder of the essay is structured as follows. In Section 2, we examine relevant research on federated learning and the classification of medicinal plants. We outline our federated learning algorithm and the used dataset for classifying medicinal plants in Section 3 of this paper. We give experimental findings and contrast the effectiveness of federated learning with different models and hyper-parameters in Section 4. We wrap up the ramifications of our findings in Section 5 and suggest ideas for new research trajectories.

2. Related Works

We employ federated machine learning algorithms to a medicinal plant dataset in order to observe the resulting effect. In almost previous research, the majority of works in federated learning utilize canonical datasets such as MNIST, CIFAR-10, and their variants, which contributes to a negative bias. In particular, this lack of generalization can prevent external individuals or organizations from utilizing federated learning in their products or service solutions, as they lack solid evidence that all research conclusions are independent of domain data or classifier architectures.

Since the early 2000s, a number of concepts regarding the partitioning of computing tasks have been explored. On structured perceptron, iterative parameter mixing implements the concept that most closely resembles how the federated learning technique is constructed [9]. In addition, some publications investigate distributed optimization methods [2, 24]. These works focus solely on reducing complexity and maximizing available hardware resources in

order to accelerate the learning process (data is gathered at one location). Federated Learning is the result of integrating previous works in response to the need for a model that enables the security and use of massive data on end devices [10]. In this new context, there are inherent challenges (we follow these challenges in directing our experiments, which will be presented in greater detail in subsequent sections): (1) privacy concerns; (2) the disparity in client data regarding size, feature space, and data distribution; (3) different hardware specifications; and (4) convergence assurance when compared to a centralized situation.

FedAvg [10] illustrates that client diversity is the most critical factor affecting our performance. Some recent investigations have attempted to address this issue, but they are not exhaustive. In spite of the fact that FedAvg is an empirical technique that functions well in specific contexts under the condition that hyper-parameters are properly tuned, more recent theoretical works support the robustness of this method [22, 23]. However, the authors presume that every device participates in each round of the process and that the used solver is typically predefined (either SGD or GD). Exposing a client's data to other clients or to the coordinator is a strategy for addressing the heterogeneous issue. Nonetheless, this imposes a significant stress on network bandwidth (especially in environments with expensive network connections) and simultaneously violates privacy standards. FedProx [7] provides a more comprehensive theoretical framework for handling heterogeneous data than previous works. Through a mechanism that permits some clients to submit their truncated parameters, the authors also accommodate for the disparity in computational capabilities between clients.

Fig. 2: The demonstration of VNPlant-200 dataset.

Numerous researchers are drawn to the identification of medicinal plants due to its widespread applications in both the medicinal community and industry. Regarding datasets, the majority of works rely on their own self-collected datasets, which typically offer distinct properties because each nation has a unique biologic ecosystem. This com-

plicates the process of comparing attained results for the purpose of leveraging existing models, as collectors utilize various lighting, perspectives, sizes, and backgrounds when taking photographs. Currently employed leaf recognition datasets include Flavia [20], Swedish Leaf [16], ICL [19], Leafsnap [5]. The majority of the images were captured in controlled environments, and each represents a distinct group of plants. Evidently, identifying a single leaf in indoor conditions is a far away from identifying a plant in an outdoor setting captured by a handheld device. Several papers on medicinal plants from India and Southeast Asia have been proposed with different datasets [14, 6, 1, 18, 11]. Leaf detection could be utilized to improve overall performance; it requires image preprocessing, image enhancement, or even localization and segmentation. Gao and Lin [3] employ OTSU, an effective segmentation algorithm, to increase their accuracy to 99.9%. Typical feature extractors include HOG, LBP, the transform technique, and deep learning models.

VNPlant-200 [13] is regarded as the first publicly available actual dataset on Vietnamese herbs. The dataset includes 20,000 images of 200 species, with 12,000 used for training and the remainder for testing. The images are quite challenging due to the fact that it stimulates outdoor perspective with a variety of noise objects and varying points of view. Using SIFT and SURF feature extractors in conjunction with Random Forest classifier yields modest results as a baseline [13]. In [12], the author adopted multiple CNN classifiers, including VGG, Inception V3, MobileNetv2, Resnet50, DenseNet, and Xception, which significantly improves accuracy. Another group extends their experiments to numerous state-of-the-art classification backbone models and provides a tuning framework for hyper parameter. In addition, they conduct time-efficient comparisons in their task.

3. Methods

3.1. Dataset

The VNPlant-200 dataset [13] is utilized in this study to examine how well the federated learning architecture performs when classifying medicinal plants. Figure 2 demonstrates several medicinal plant samples of VNPlant-200. With a percentage of 50%, 10%, and 40%, respectively, the original dataset is separated into training, validation, and testing sets. Following that, the training images are dispersed to 10 clients using either the independent and identical distribution (IID) method or the non-independent and identical distribution (Non-IID) method. In the IID technique, clients are randomly assigned training data, resulting in data that is distributed similarly across all clients. Instead, the Non-IID technique sorts medicinal plants according to their labels before seeding the data into clients in the appropriate sequence. When using federated learning, the second strategy might reflect a heterogeneous property of decentralize data in the real world. The process of identifying medicinal plants would be more difficult than earlier similar efforts due to the diversity distribution among each client, and this would provide a new avenue for classification optimization.

3.2. Federated Learning Frameworks For Classification

The suggested medicinal plant identification frameworks utilizing federated learning include two key components: classifiers and federated learning algorithms. The demonstration of our federated learning systems is shown in Figure xx. Four contemporary deep learning architectures, namely VGG16 [15], ResNet50 [4], ConvNext [8], and MaxVit [17], are incorporated into the framework to enhance identification performance for the classification models. In the context of federated learning, at each round of communication, the classifier parameters of trained clients are sent to the central server, which then employs federated algorithms as an aggregation method for handling clients' parameters in order to update the global model. Figure 1 illustrates how a federated learning system works.

FedAvg [10] is based on a basic but effective concept. A C portion of clients would participate in the training procedure during each communication round. The located data would be looped through E epochs and B batch size for each client. After local tasks have been completed, the weights of each classifier will be averaged to update all client models. However, arbitrarily averaging the model weights could result in an unstable training process if the difference between training data from each communication round is significant. The FedProx [7] algorithm may improve classification performance through a more stable coverage process by incorporating proximal terms into loss functions in order to solve this issue.

4. Experimental Results

Many experiments are conducted to optimize federated learning framework for the best medicinal plants classification performance in a fixed number of communication rounds. To optimize federated learning framework for medicinal plant categorization in a fixed number of communication rounds, many experiments are done. All of the experiments are executed on Google Colab and require 1000 computing units, which is equivalent to 500 hours of training.

In the initial phase, the objective of tuning experiments is to determine appropriate values for C, B, and E using the baseline framework of VGG16 and FedAVg as a classifier and federated learning algorithm, respectively. Table 1 and Figure 3 displays the framework's medicinal plant identification using VGG16 and FedAvg with $B = 10$, $E = 5$, and increasing C values after 10, 20, 50, and 100 communication cycles. hen more clients are involved in each training round at once, the categorization performance improves. In addition, the extent of influence between IID and Non-IID data differs. Specifically, on Non-IID data, the classification results improve more than IID data on each increment value of C, which can be explained by the unique data distribution of each Non-IID client, but the data distribution of IID clients is similar to the worldwide distribution. For the sake of computation, subsequent experiments fix C to 0.2 and tune additional variables such as B, E, and the classifier.

Table 2 and Figure 4 demonstrates the classification performance of the proposed framework with varying values of B and E. When increasing the batch size from $B = 10$ to $B = 16$, the highest accuracy for inspected rounds also improves substantially. Following 100 rounds, the accuracy of IID data grew by 0.37%, from 88.56% to 88.93%, while the accuracy of Non-IID data climbed by 0.95%, from 67.81% to 68.76%. However, consistently increasing B to 32 does not result in a significant improvement comparable to $B = 16$. Thus, $B = 16$ would be an optimal value of B in the federated learning framework for medicinal plant classification. To avoid over-fitting of the local model during training progress, small values of epoch E are used in the experiments. For $E = 1$ and $E = 2$, there is no improvement in the training stage for either IID or Non-IID data, so the optimal number of epochs is $E = 5$.

After determining the most suitable hyper-parameters for the framework, a number of contemporary deep learning networks are used as classifiers to determine which could yield the highest accuracy. These experimental outcomes are displayed in Table 3 and Figure 5. Using ConvNext as a classification model considerably increases the final accuracy of IID results from 88.93% to 94.51%. In the meantime, after 100 communication cycles, ResNet50 is the best model for classifying Non-IID medicinal plant data with 82.65% accuracy, a 13.92% improvement over VGG16's 68.76% accuracy. Despite the suggested framework achieves excellent performance with FedAvg on IID data, with a peak of

C	IID				Non-IID			
	10	20	50	100	10	20	50	100
0.1	68.34	77.84	84.95	85.56	10.44	12.81	20.00	31.80
0.2	77.08	82.90	86.80	88.56	33.39	41.35	60.19	67.81
0.3	80.34	85.15	88.04	89.24	38.13	53.61	70.65	74.68
0.5	81.71	86.76	89.09	89.09	51.73	66.40	77.71	81.28

Table 1: Classification results of VGG16, FedAvg with $B = 10$, $E = 5$ and different C

E	B	IID				Non-IID			
		10	20	50	100	10	20	50	100
5	10	77.08	82.90	86.80	88.56	33.39	41.35	60.19	67.81
5	16	78.48	83.41	87.59	88.93	31.61	41.59	58.60	68.76
5	32	79.38	84.13	86.69	88.28	31.51	44.14	57.39	66.66
1	10	55.60	70.00	81.20	85.71	21.49	36.04	48.56	63.11
2	10	65.03	78.36	84.75	88.64	26.96	38.33	58.53	67.34

Table 2: Tuning results of VGG16 and FedAvg with $C = 0.2$

94.51% after 100 communication rounds, the task of classifying Non-IID remains difficult, with a final accuracy of just

Model	IID				Non-IID			
	10	20	50	100	10	20	50	100
VGG16	78.48	83.41	87.59	88.93	31.61	41.59	58.60	68.76
ConvNext	86.40	91.29	93.59	94.51	30.86	48.15	68.11	73.09
ResNet50	82.73	87.93	91.94	93.10	34.51	48.15	72.85	82.65
MaxVit	79.41	88.64	92.65	94.01	36.76	43.08	69.79	76.33

Table 3: Classification results on different models using FedAvg with $C = 0.2$, $B = 16$, and $E = 5$

Muy	Non-IID			
	10	20	50	100
0	34.51	48.15	72.85	82.65
1	35.48	50.00	73.23	82.95
0.1	34.76	48.48	73.13	82.37
0.01	34.34	50.93	73.10	82.71
0.001	35.24	49.60	73.81	82.41

Table 4: Medical plants classification results with FedProx, ResNet50, $C = 0.2$, $B = 16$, and $E = 5$

82.65%. Individual clients' disparate data distributions slow down the convergence of classification models and hinder global models from correctly representing the distribution of data. FedProx is therefore anticipated to maintain the training process' stability by including a proximal term in the loss function, which may be managed by changing the value of μ. The results of the federated learning framework utilizing ResNet50 and FedProx with diverse μ values are presented in Table 4 and Figure 6. In comparison to the findings of FedAvg (μ=0), all FedProx tests produce superior results, reaching a peak at $\mu = 1$ with 0.38% improved accuracy after 50 rounds and 0.30% improved accuracy after 100 rounds.

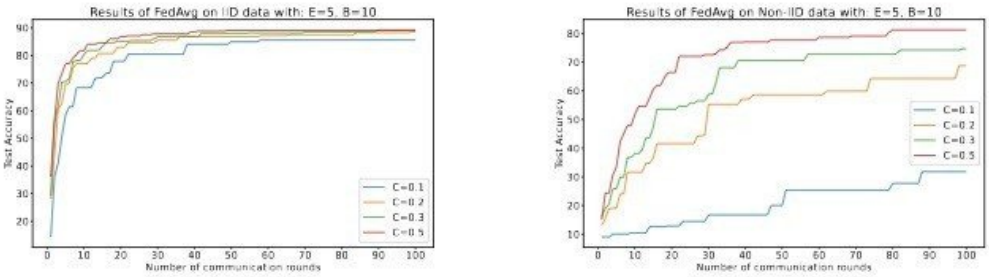

(a) IID data (b) Non-IID data

Fig. 3: Classification results of VGG16, FedAvg with B = 10, E = 5 and different C

5. Conclusion

In this work, the usefulness of federated learning for medicinal plant classification was investigated utilizing both IID and Non-IID data. FedAvg and FedProx algorithms were utilized to train a deep learning classifier on a large dataset of medicinal plant images that were distributed across multiple participating devices without the need to share data. The performance of our federated learning system was enhanced by adjusting hyper-parameters including the batch size B, number of epochs E, classifier model, and control value of proximal term mu. Additionally, we have shown how FedProx outperforms FedAvg in terms of accelerating convergence and strengthening the training process, especially apparent for Non-IID data. In the end, after 100 communication rounds, the fantastic performance

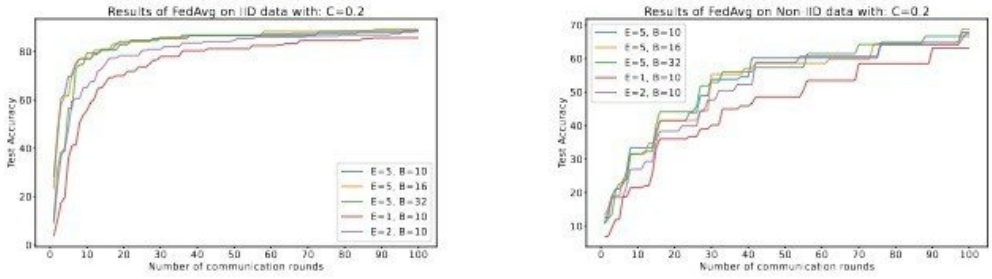

(a) IID data (b) Non-IID data

Fig. 4: Tuning results of VGG16 and FedAvg with C = 0.2

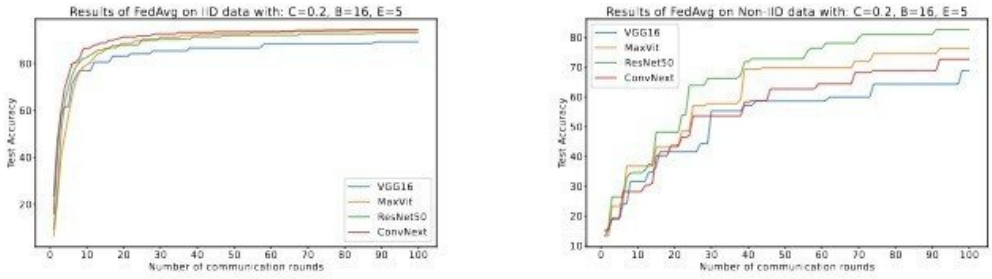

(a) IID data (b) Non-IID data

Fig. 5: Classification results on different models using FedAvg with $C = 0.2$, $B = 16$, and $E = 5$

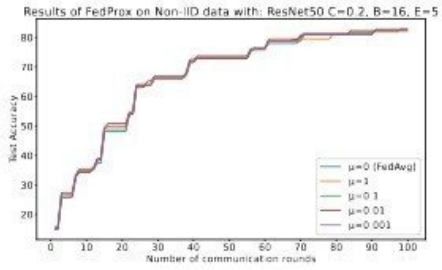

Fig. 6: Medical plants classification results with FedProx, ResNet50, $C = 0.2$, $B = 16$, and $E = 5$

of the ideal framework helped enhance 5.95% accuracy on IID data and 14.84% accuracy on Non-IID data compared to the baseline design. Moreover, we discovered that the efficacy of our federated learning system with Non-IID data was inferior to that with IID data. The performance of the federated learning approach may suffer as a result of the dissemination of Non-IID data, according to this.

Overall, the findings of this study indicate that federated learning is a promising approach for the classification of medicinal plants and other applications where privacy and data security are crucial. Nonetheless, the efficacy of the federated learning approach may be impacted by the data distribution, particularly when Non-IID data are involved. Future research could investigate the use of other, more complex federated learning algorithms and further hyper-parameter optimization to enhance the system's efficacy on Non-IID data.

References

[1] Arun, C.H., Durairaj, D.C., 2017. Identifying medicinal plant leaves using textures and optimal colour spaces channel. Jurnal Ilmu Komputer dan Informasi 10, 19. doi:10.21609/jiki.v10i1.405.

[2] Dean, J., Corrado, G., Monga, R., Chen, K., Devin, M., Mao, M., aurelio Ranzato, M., Senior, A., Tucker, P., Yang, K., Le, Q., Ng, A., 2012. Large scale distributed deep networks, Curran Associates, Inc. URL: https://proceedings.neurips.cc/paper_files/paper/2012/file/6aca97005c68f1206823815f66102863-Paper.pdf.

[3] Gao, L., Lin, X., 2018. A method for accurately segmenting images of medicinal plant leaves with complex backgrounds. Computers and Electronics in Agriculture 155, 426–445. doi:10.1016/j.compag.2018.10.020.

[4] He, K., Zhang, X., Ren, S., Sun, J., 2015. Deep residual learning for image recognition .

[5] Kumar, N., Belhumeur, P.N., Biswas, A., Jacobs, D.W., Kress, W.J., Lopez, I.C., Soares, J.V.B., 2012. Leafsnap: A Computer Vision System for Automatic Plant Species Identification. pp. 502–516. doi:10.1007/978-3-642-33709-3_36.

[6] Le, T.L., Tran, D.T., Hoang, V.N., 2014. Fully automatic leaf-based plant identification, application for vietnamese medicinal plant search, ACM Press. pp. 146–154. doi:10.1145/2676585.2676592.

[7] Li, T., Sahu, A.K., Zaheer, M., Sanjabi, M., Talwalkar, A., Smith, V., 2018. Federated optimization in heterogeneous networks .

[8] Liu, Z., Mao, H., Wu, C.Y., Feichtenhofer, C., Darrell, T., Xie, S., 2022. A convnet for the 2020s, IEEE. pp. 11966–11976. doi:10.1109/CVPR52688.2022.01167.

[9] McDonald, R., Hall, K., Mann, G., 2010. Distributed training strategies for the structured perceptron, in: Human Language Technologies: The 2010 Annual Conference of the North American Chapter of the Association for Computational Linguistics, Association for Computational Linguistics, Los Angeles, California. pp. 456–464. URL: https://aclanthology.org/N10-1069.

[10] McMahan, H.B., Moore, E., Ramage, D., Hampson, S., y Arcas, B.A., 2016. Communication-efficient learning of deep networks from decentralized data URL: http://arxiv.org/abs/1602.05629.

[11] Minh, T.D., Minh, T.T., Quoc, T.N., Hoang, V.T., 2023. Features Extraction Based on Sota Models for Medicinal Plant Images Recognition. pp. 465–473. doi:10.1007/978-3-031-27524-1_44.

[12] Quoc, T.N., Hoang, V.T., 2020. Medicinal plant identification in the wild by using cnn, IEEE. pp. 25–29. doi:10.1109/ICTC49870.2020.9289480.

[13] Quoc, T.N., Hoang, V.T., 2021. VNPlant-200 – A Public and Large-Scale of Vietnamese Medicinal Plant Images Dataset. pp. 406–411. doi:10.1007/978-3-030-49264-9_37.

[14] Sainin, M.S., Ghazali, T.K., Alfred, R., 2012. Malaysian Medicinal Plant Leaf Shape Identification and Classification. Master's thesis. URL: http://www.kmice.cms.net.my/.

[15] Simonyan, K., Zisserman, A., 2014. Very deep convolutional networks for large-scale image recognition .

[16] Söderkvist, O.J.O., 2001. Computer Vision Classification of Leaves from Swedish Trees. Master's thesis.

[17] Tu, Z., Talebi, H., Zhang, H., Yang, F., Milanfar, P., Bovik, A., Li, Y., 2022. Maxvit: Multi-axis vision transformer .

[18] Vo, A.H., Dang, H.T., Nguyen, B.T., Pham, V.H., 2019. Vietnamese herbal plant recognition using deep convolutional features. International Journal of Machine Learning and Computing 9, 363–367. doi:10.18178/ijmlc.2019.9.3.811.

[19] Wang, B., Gao, Y., Sun, C., Blumenstein, M., Salle, J.L., 2017. Can walking and measuring along chord bunches better describe leaf shapes?, IEEE. pp. 2047–2056. doi:10.1109/CVPR.2017.221.

[20] Wu, S.G., Bao, F.S., Xu, E.Y., Wang, Y.X., Chang, Y.F., Xiang, Q.L., 2007. A leaf recognition algorithm for plant classification using probabilistic neural network, IEEE. pp. 11–16. doi:10.1109/ISSPIT.2007.4458016.

[21] Yang, Q., Liu, Y., Chen, T., Tong, Y., 2019. Federated machine learning. ACM Transactions on Intelligent Systems and Technology 10, 1–19. doi:10.1145/3298981.

[22] Yu, H., Jin, R., Yang, S., 2019a. On the linear speedup analysis of communication efficient momentum sgd for distributed non-convex optimization .

[23] Yu, H., Yang, S., Zhu, S., 2019b. Parallel restarted sgd with faster convergence and less communication: Demystifying why model averaging works for deep learning. Proceedings of the AAAI Conference on Artificial Intelligence 33, 5693–5700. doi:10.1609/aaai.v33i01.33015693.

[24] Zhang, S., Choromanska, A.E., LeCun, Y., 2015. Deep learning with elastic averaging sgd, Curran Associates, Inc. URL: https://proceedings.neurips.cc/paper_files/paper/2015/file/d18f655c3fce66ca401d5f38b48c89af-Paper.pdf.

Table A1. Original results from proposed work when evaluating **MNIST** with $\boldsymbol{E = 1}$ on 2NN and $\boldsymbol{E = 1}$ on CNN. Each cell represents the communication cost needed to a respective model to achieve desired test-set accuracy. (99% with CNN and 97% with 2NN). Five attempts did not convergence in time.

	IID		NON-**IID**	
C	$\boldsymbol{B = \infty}$	$\boldsymbol{B = 10}$	$\boldsymbol{B = \infty}$	$\boldsymbol{B = 10}$
			2NN	
0.0	1455	316	4278	3275
0.1	1474	87	1796	664
0.2	1658	77	1528	619
0.5	—	75	—	443
1.0	—	70	—	380
			CNN	
0.0	387	50	1181	956
0.1	339	18	1100	206
0.2	337	18	978	200
0.5	164	18	1067	261
1.0	246	16	—	97

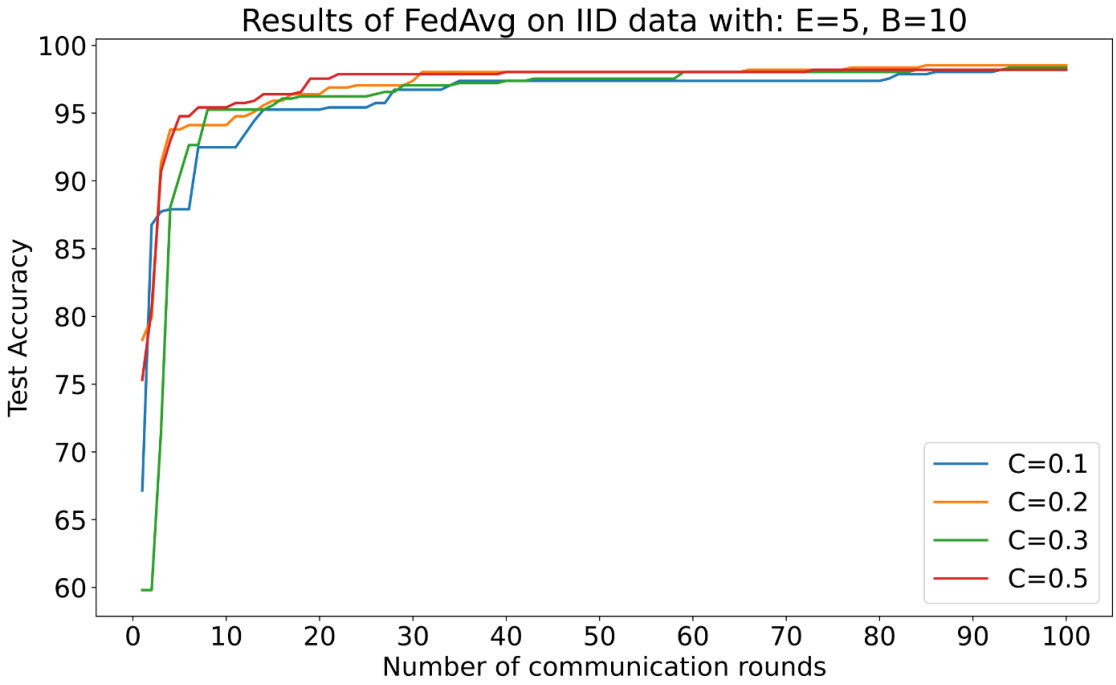

Figure A1. Plots on test-set accuracy over time on IID Brain Tumor Dataset with different client fraction hyper parameter. The figure only shows the **FedAvg** scores.

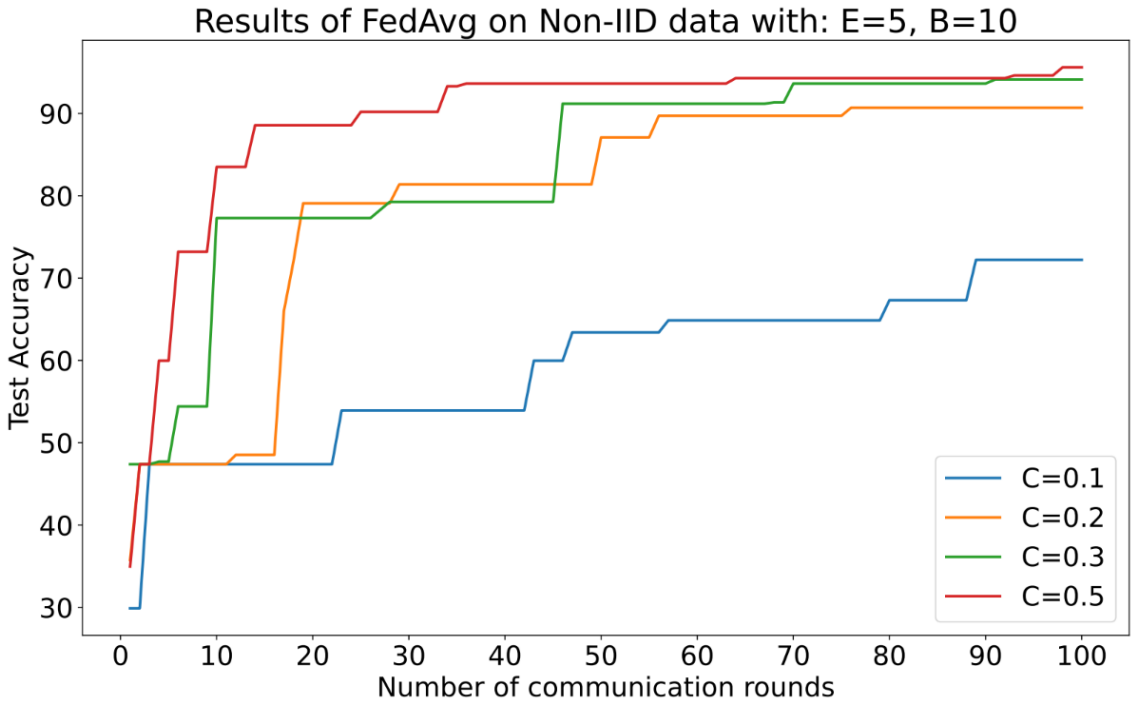

Figure A2. Plots on test-set accuracy over time on non-**IID** Brain Tumor Dataset with different client fraction hyper parameter. The figure only shows the **FedAvg** scores.

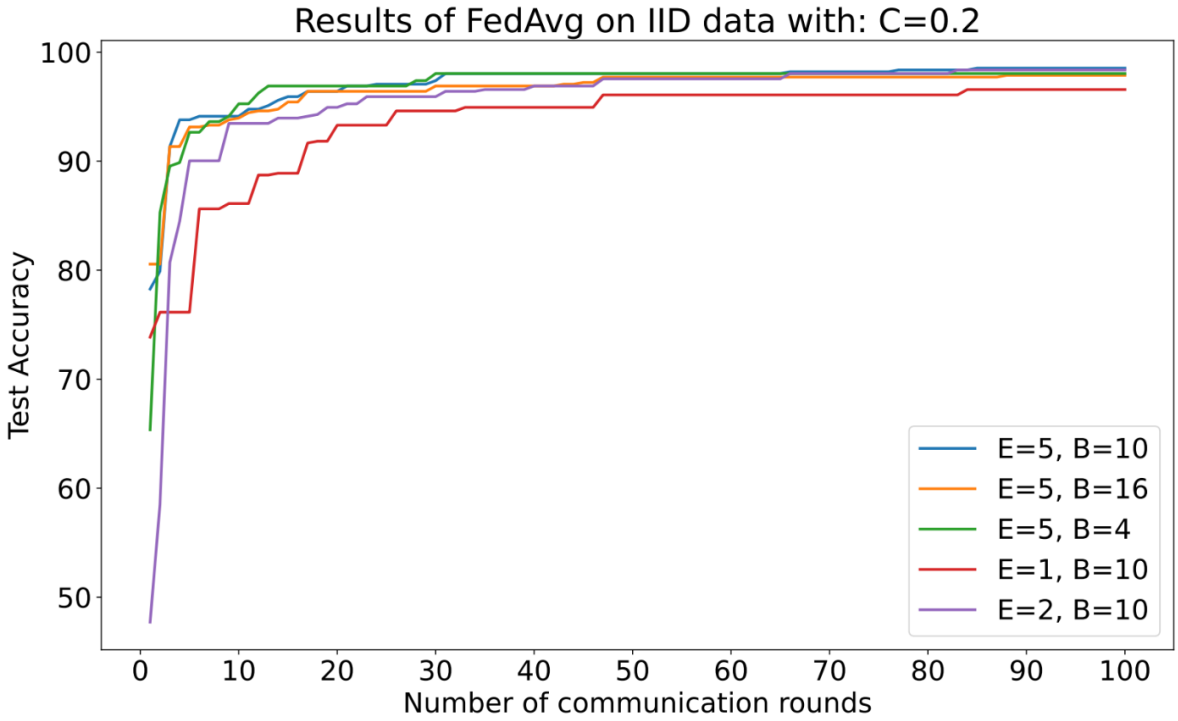

Figure A3. The effect of different local computing works on each entry with **FedAvg**. Here we fix C=0.2. The **IID** version of Brain Tumor dataset is used.

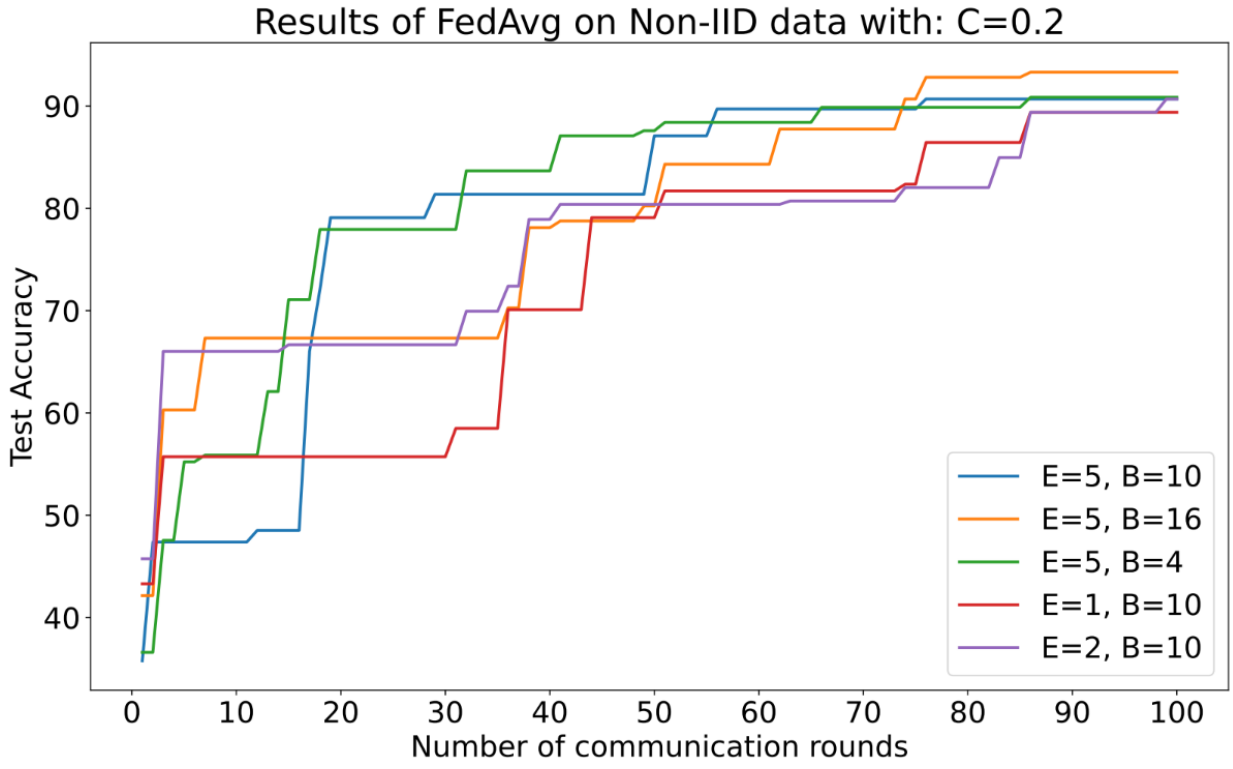

Figure A4. The effect of different local computing works on each entry with **FedAvg**. Here we fix C=0.2. The non-**IID** version of Brain Tumor dataset is used.

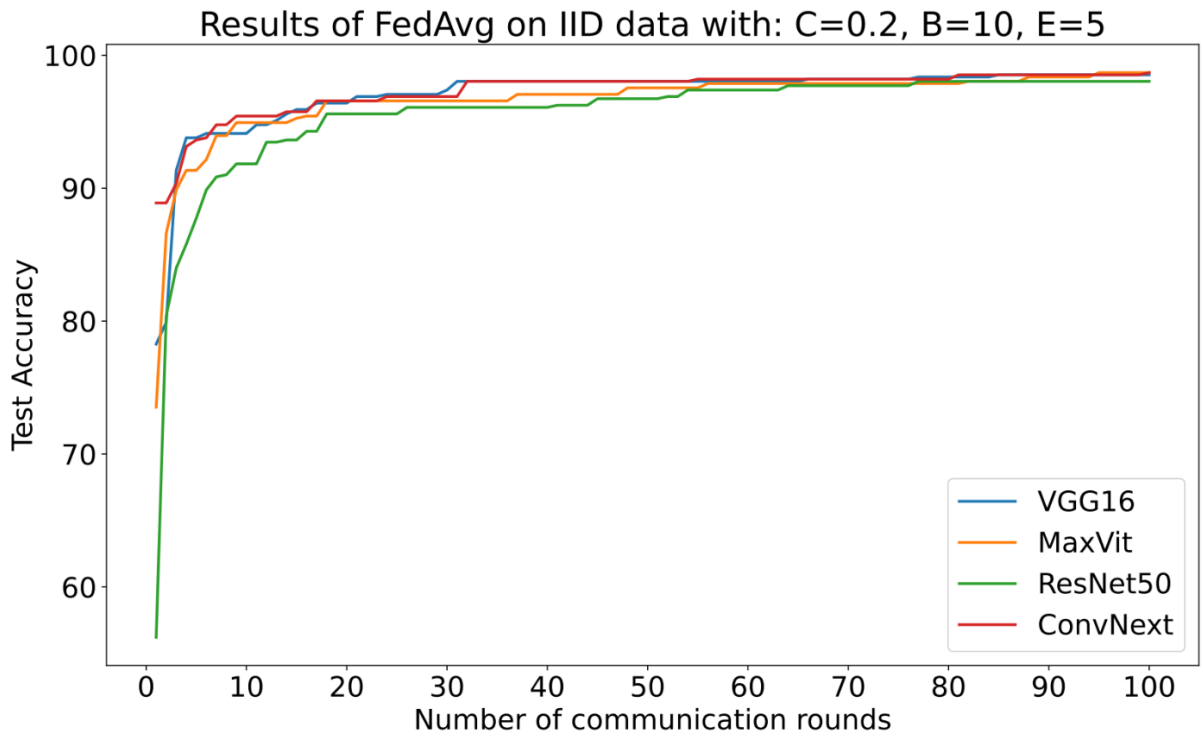

Figure A5. The classifier selection impact is inspected here with **IID** Brain Tumor dataset.

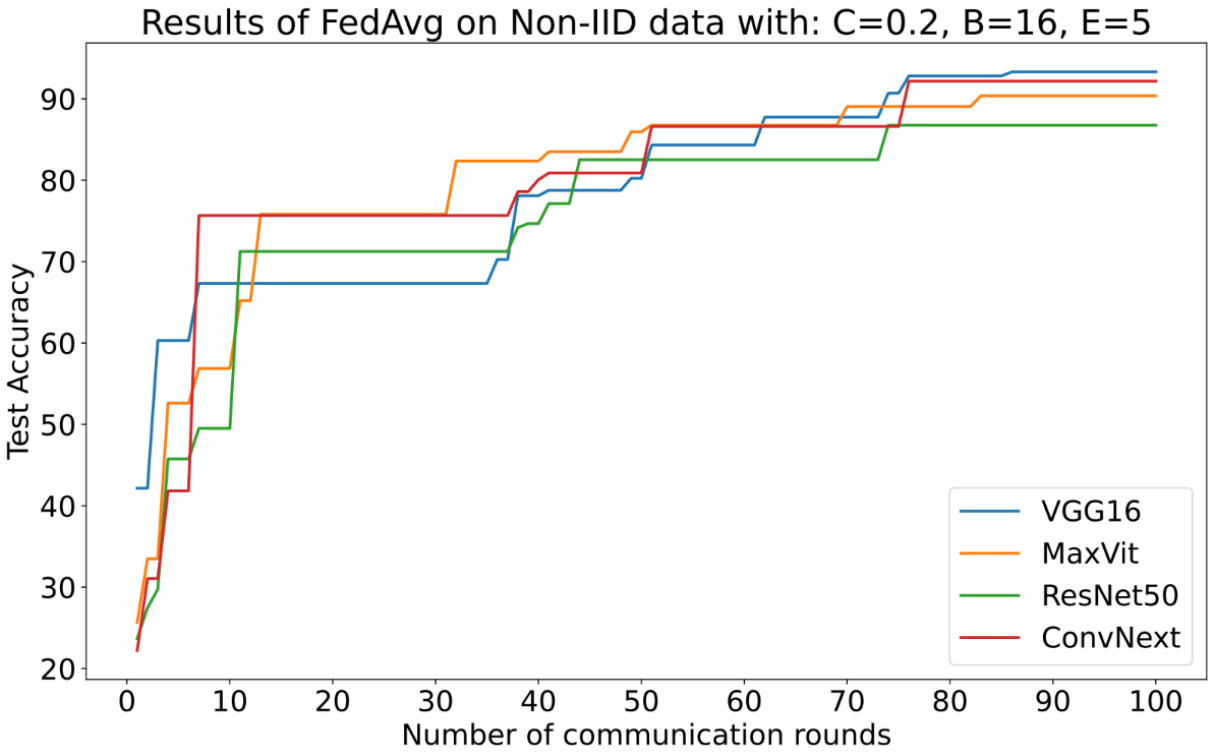

Figure A6. The classifier selection impact is inspected here with non-**IID** Brain Tumor dataset.

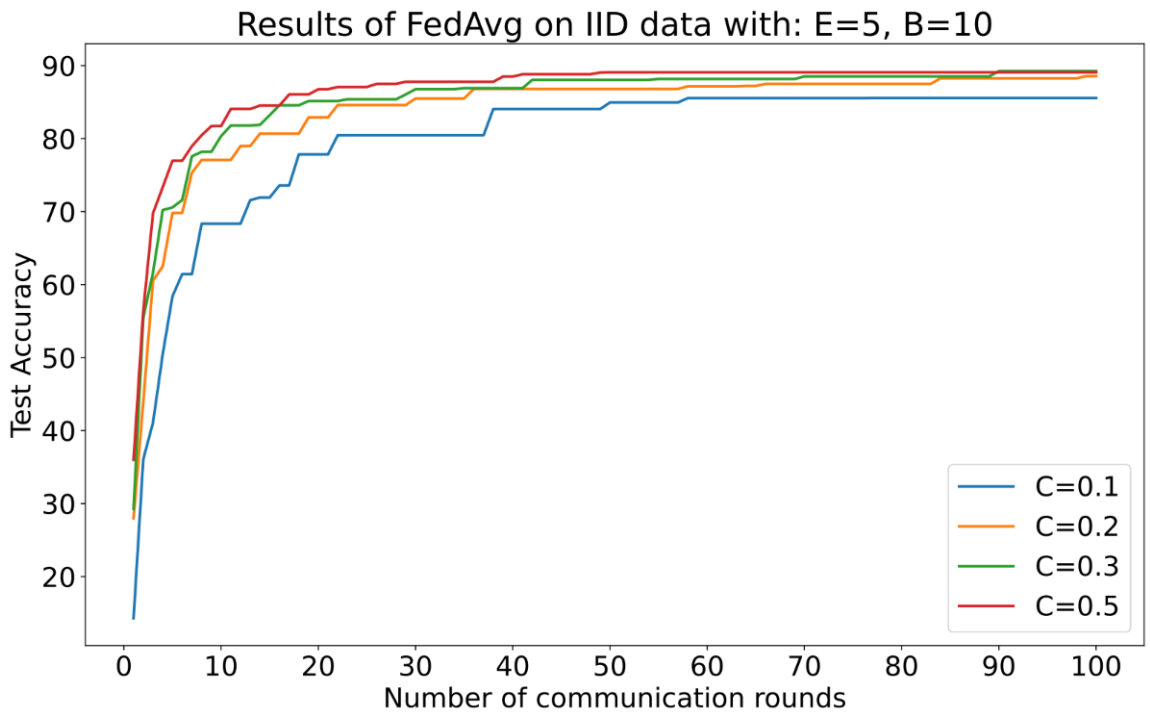

Figure A7. FedAvg on the **IID** version of **VNPlant-200** dataset using **VGG16** classifier.

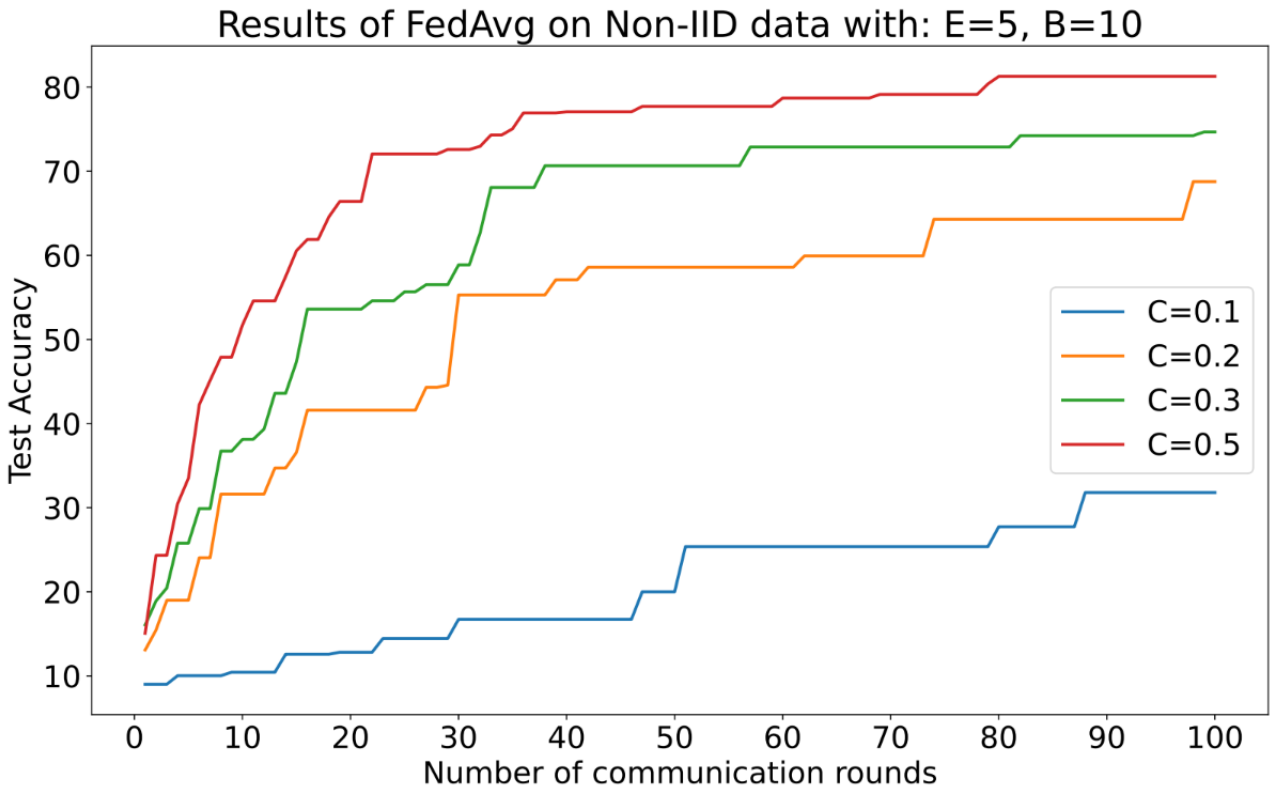

Figure A8. FedAvg on the non-**IID** version of **VNPlant-200** dataset using **VGG16** classifier.

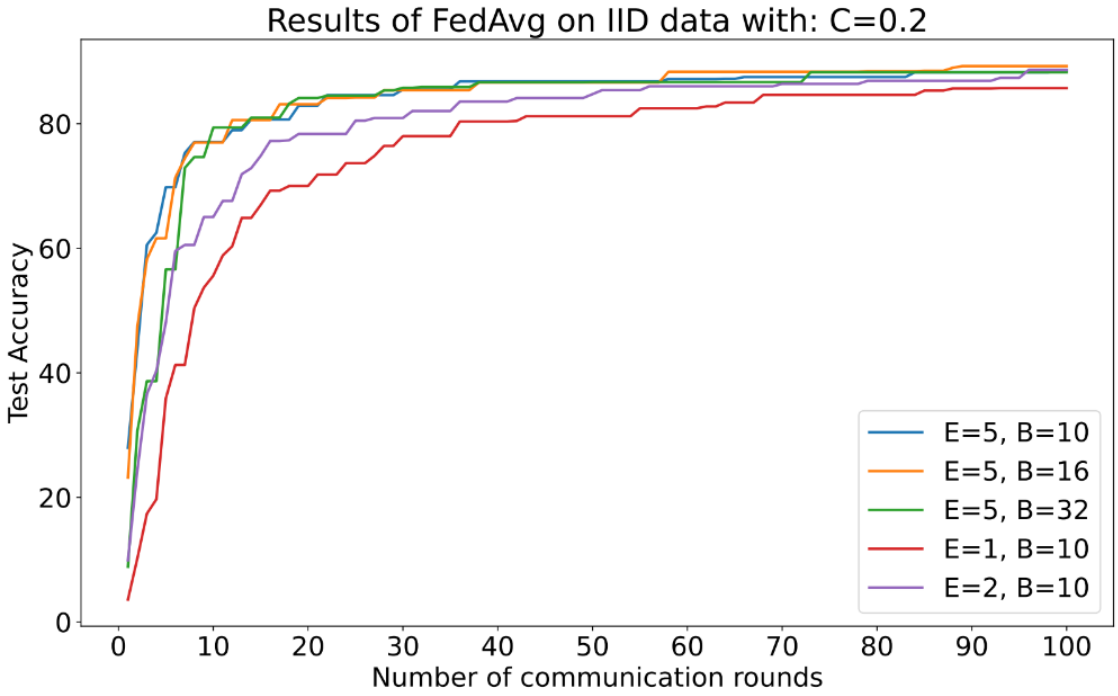

Figure A9. The effect of different local computing works on each entry with **FedAvg**. Here we fix C=0.2. The **IID** version of **VNPlant-200** dataset is used. (**VGG16 classifier)**

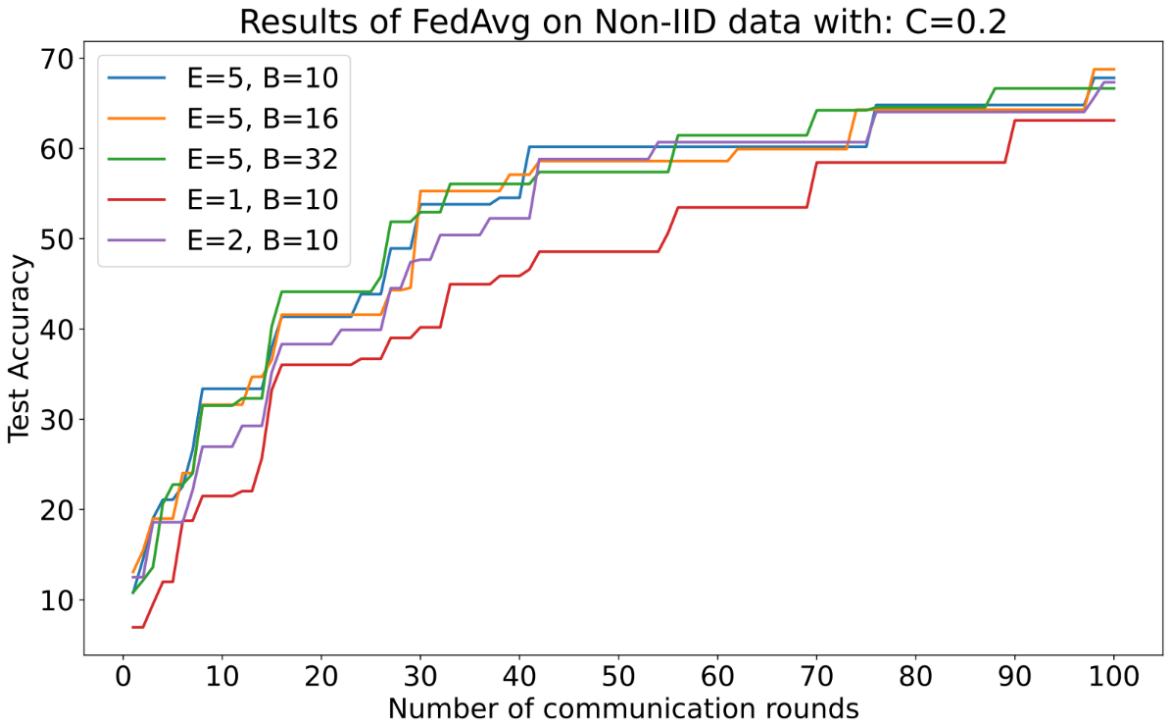

Figure A10. The effect of different local computing works on each entry with **FedAvg**. Here we fix C=0.2. The **IID** version of **VNPlant-200** dataset is used. (**VGG16 classifier)**

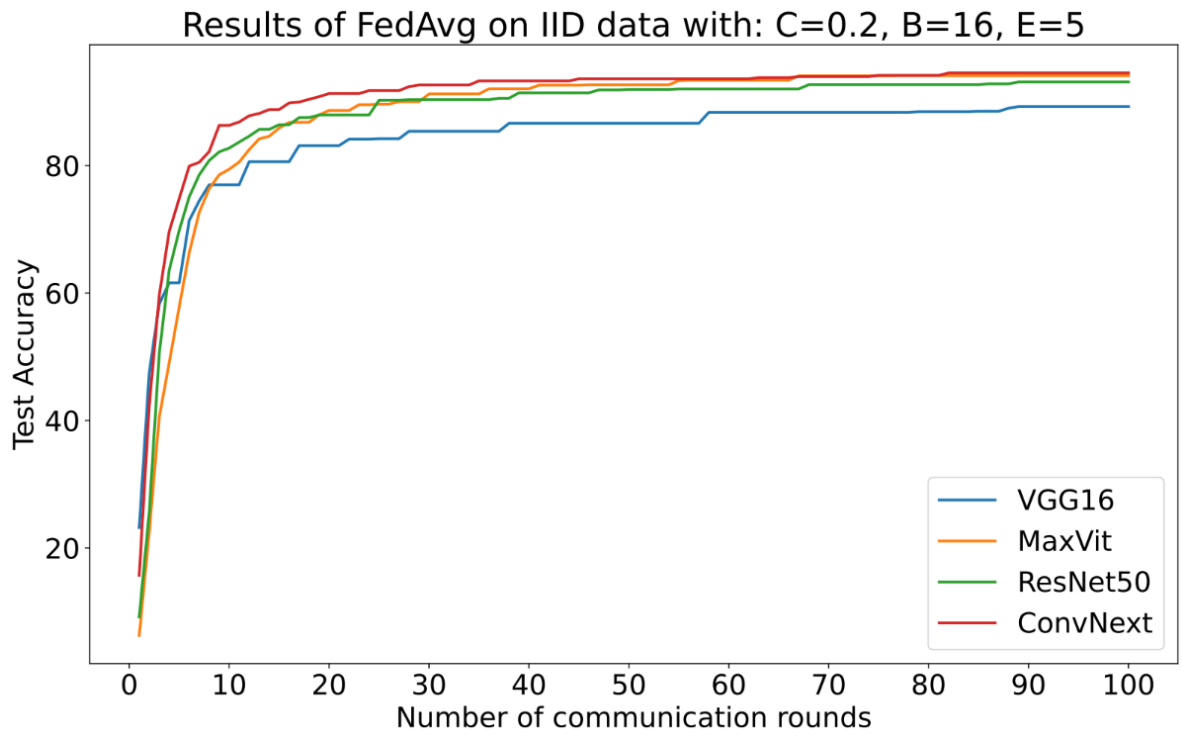

Figure A11. The classifier selection impact is inspected here with **IID VNPlant-200** dataset.

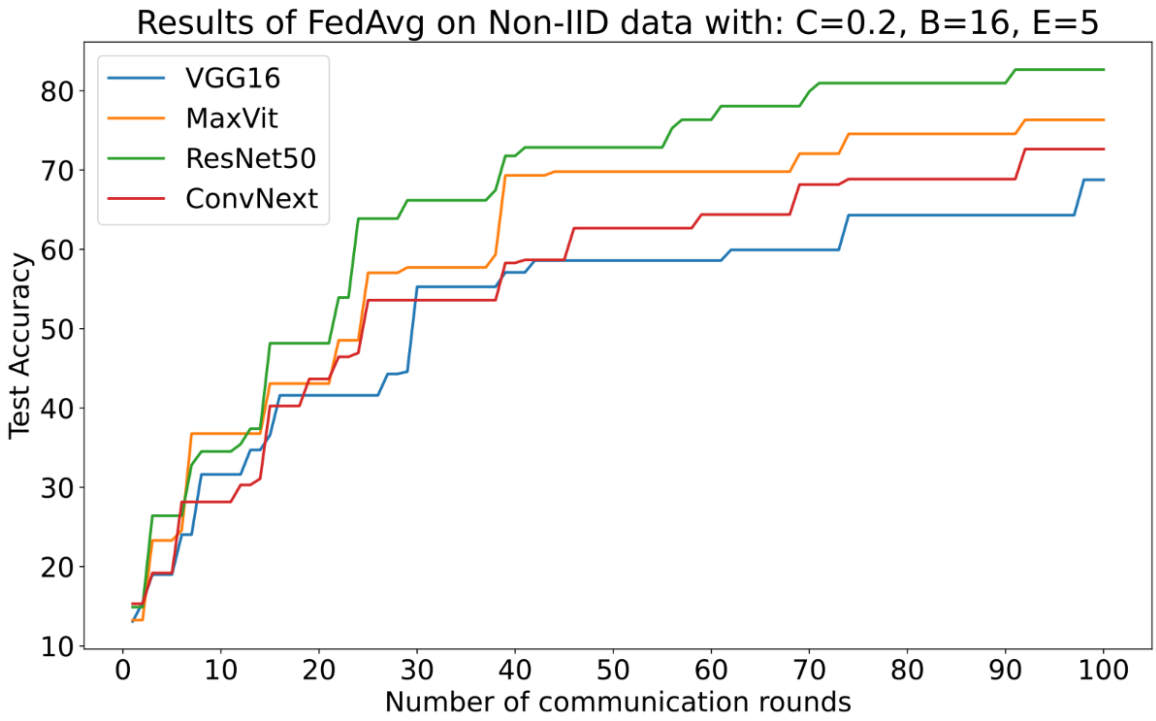

Figure A12. The classifier selection impact is inspected here with non-**IID VNPlant-200** dataset.